Acta Neuropathol (2011) 121:113–134
DOI 10.1007/s00401-010-0700-3

REVIEW

Cellular and sub-cellular pathology of animal prion diseases: relationship between morphological changes, accumulation of abnormal prion protein and clinical disease

Martin Jeffrey · Gillian McGovern · Silvia Sisó · Lorenzo González

Received: 4 February 2010 / Revised: 4 May 2010 / Accepted: 19 May 2010 / Published online: 8 June 2010

Abstract The transmissible spongiform encephalopathies (TSEs) or prion diseases of animals are characterised by CNS spongiform change, gliosis and the accumulation of disease-associated forms of prion protein (PrP^d). Particularly in ruminant prion diseases, a wide range of morphological types of PrP^d depositions are found in association with neurons and glia. When light microscopic patterns of PrP^d accumulations are correlated with sub-cellular structure, intracellular PrP^d co-localises with lysosomes while non-intracellular PrP^d accumulation co-localises with cell membranes and the extracellular space. Intracellular lysosomal PrP^d is N-terminally truncated, but the site at which the PrP^d molecule is cleaved depends on strain and cell type. Different PrP^d cleavage sites are found for different cells infected with the same agent indicating that not all PrP^d conformers code for different prion strains. Non-intracellular PrP^d is full-length and is mainly found on plasma-lemmas of neuronal perikarya and dendrites and glia where it may be associated with scrapie-specific membrane pathology. These membrane changes appear to involve a redirection of the predominant axonal trafficking of normal cellular PrP and an altered endocytosis of PrP^d. PrP^d is poorly excised from membranes, probably due to increased stabilisation on the membrane of PrP^d complexed with other membrane ligands. PrP^d on plasma-lemmas may also be transferred to other cells or released to the extracellular space. It is widely assumed that PrP^d accumulations cause neurodegenerative changes that lead to clinical disease. However, when different animal prion diseases are considered, neurological deficits do not correlate well with any morphological type of PrP^d accumulation or perturbation of PrP^d trafficking. Non-PrP^d-associated neurodegenerative changes in TSEs include vacuolation, tubulovesicular bodies and terminal axonal degeneration. The last of these correlates well with early neurological disease in mice, but such changes are absent from large animal prion disease. Thus, the proximate cause of clinical disease in animal prion disease is uncertain, but may not involve PrP^d.

Keywords Prion · Electron microscopy · Neurodegeneration · Scrapie · BSE · Trafficking

M. Jeffrey (✉) · G. McGovern · S. Sisó · L. González
Veterinary Laboratories Agency, Lasswade Laboratory, Pentlands Science Park, Bush Loan, Penicuik, Midlothian EH26 0PZ, UK
e-mail: m.jeffrey@vla.defra.gsi.gov.uk

Introduction

Naturally occurring transmissible spongiform encephalopathies (TSEs) or prion diseases of animals include scrapie of sheep and goats, bovine spongiform encephalopathy (BSE) of cattle, chronic wasting disease of several free living and captive deer species [121] and transmissible mink encephalopathy of captive mink [113]. BSE-related disorders have been described in domestic cats [126] in exotic felids [88], in ruminants in zoological collections [32, 85] and also in man (variant Creutzfeldt–Jakob disease). Animal prion diseases have been extensively transmitted within and between species. Most intra-species transmissions have been performed in sheep and two well-characterised sources that can be viewed as strains—SSBP/1 and CH1641—have been described [37, 62]. Most studies of inter-species transmissions have involved the isolation of sheep scrapie in mice or voles. Numerous scrapie strains have been recognised in mice following passage of sheep scrapie at limiting dilutions [21], but whether such strains

are mutations or adaptations of the original source material as a reflection of the host–strain interaction remains uncertain. In contrast, cattle BSE has been cloned in mice and has also been transmitted to goats, sheep, deer and pigs as a single unique strain [14, 18]. Fewer well-characterised isolates have been identified from chronic wasting disease transmissions [57], but two well-characterised strains known as hyper and drowsy have been isolated on serial passage of transmissible mink encephalopathy into hamsters [12]. For the purpose of this review we define a strain as a type of TSE which has consistent clinical, pathological, biochemical and transmission characteristics when passaged at limiting dilution within a single host species and PrP (*PRNP*) genotype. For field cases, the agents causing disease with common clinical, pathological and biochemical characteristics will be referred to as sources or isolates.

Prion diseases are typically described as having lesions of spongiform change, gliosis and neuronal loss, which are associated with accumulations of abnormal isoforms of the host encoded cell surface sialoglycoprotein prion protein (PrP or PrP^{c}). The nomenclature used in prion biology in respect to different forms of PrP is often confusing. Here, we will use the term PrP^{c} to denote those forms and localisations of PrP that are found in healthy brains. The term "disease-associated PrP" (PrP^{d}) will be used for abnormal PrP forms visualised by immunohistochemical methods in diseased brains that are absent from healthy brains. PrP^{res} describes the resistant core of abnormal PrP detected by Western blotting after partial proteolysis of detergent extracts of prion disease infected brains. Thus, PrP nomenclatures used in this review have operational definitions that do not inform on infectivity.

Within the last few years several novel prion diseases have been recognised in sheep [11], goats and cattle [22, 64]. The atypical disease variants of cattle are rare and are found sporadically within populations, but 'Nor 98' or atypical sheep scrapie is now more frequently detected in the UK sheep population than is classical scrapie and may occur with relatively high frequency in association with one particular *PRNP* polymorphism. Atypical prion diseases are readily distinguished from classical forms of disease by biochemical and pathological features. Atypical scrapie is commonly found in geographical regions and countries that do not have classical ruminant prion diseases, and affects animals with polymorphisms of the PrP (*PRNP*) gene proportionally different from those targeted by classical scrapie. Two novel cattle prion diseases have been identified and are known as L-type (or BASE) and H-type BSE [64]. Most atypical forms of ruminant prion disease are detected by active surveillance of animals with no clinical signs of disease, so that the relationships between PrP^{d} accumulation, pathology and disease are difficult to evaluate in such animals. As yet there is little data on the cellular and sub-cellular pathology of atypical sheep and cattle prion disease and, therefore, discussion of atypical forms of prion disease will be limited within this review.

We will revise knowledge of neuropathological changes of animal prion disease at cellular and at sub-cellular levels. We will describe the different forms of PrP^{d} that can be visualised by light and electron microscopy immunohistochemical techniques and discuss how the tissue accumulation of PrP^{d} is related to morphological changes at the sub-cellular level. We will further discuss the sub-cellular localisation of PrP^{c} and how the localisation of PrP^{d} informs on the conversion and trafficking of these molecules. Finally, we will consider the relationship between form and function: whether PrP^{d} or other changes found in TSEs can be related to neurological disease or to infectivity.

The nature and range of neuropathological changes

The characteristic light microscopic pathology of animal TSEs is usually described as grey matter vacuolation of neuropil (Fig. 1), astrogliosis and microglial activation, and neuronal loss. However, there is considerable variation in the extent to which these changes occur in animals. For example, many naturally occurring cases of cattle BSE and experimental SSBP/1 scrapie produce very little or no vacuolation or gliosis [8, 155]. While neuronal loss can be a prominent feature of some murine scrapie strains [33], it is generally an inconspicuous feature of ruminant TSEs. Where morphometric techniques have been used to demonstrate neuronal loss in cattle BSE, losses can be variable and inconsistent [79].

PrP^{d} accumulation is consistently (but not universally) present in field and experimental animal prion diseases. Different morphological types of PrP^{d} accumulations can be detected by immunohistochemical methods (Fig. 2). In rodents and mink, PrP^{d} accumulates in a relatively restricted range of morphological patterns, most commonly as diffuse punctuate forms and as amyloid plaques [17, 99] although intracellular, perineuronal [74] and astrocyte-associated PrP^{d} may be found in some rodent strains [38] and in a transgenic line ($Tg3Prnp^{-/-}$) engineered to express PrP^{c} only on astrocytes [131]. In contrast, individual brains of cattle [24, 139, 140, 155], deer [144] and sheep [53, 150] with prion disease have a wide range of morphological types of PrP^{d} accumulation, including intra-neuronal and intra-glial accumulations and patterns surrounding astroglia, microglia, neurons, ependyma and blood vessels [53] (Fig. 2). When the abundance and distribution of PrP^{d} types are systematically recorded in entire brains the resultant 'PrP^{d} profiles' show distinct patterns

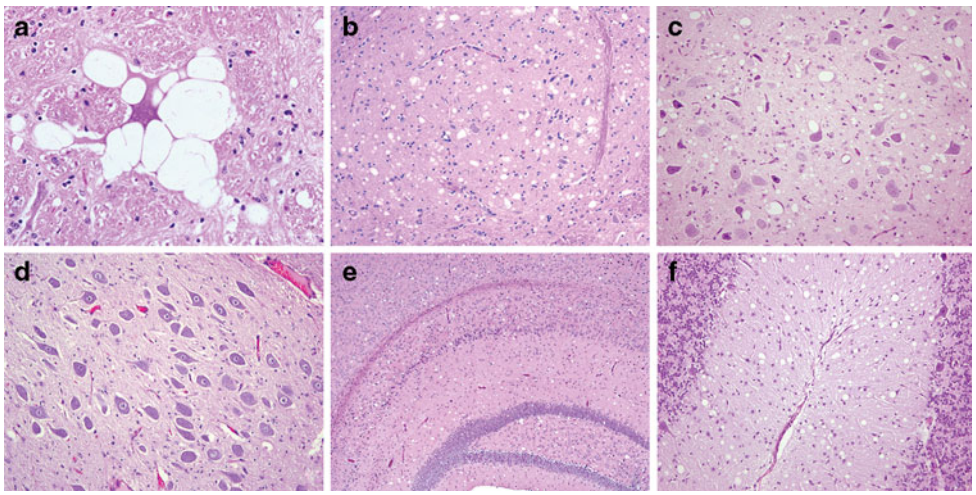

Fig. 1 Morphological forms of grey matter vacuoles. Vacuoles may form both in neuronal perikarya and in grey matter neuropil. They are not usually associated with an immune response. **a** Vestibular complex of a BSE-affected cow with loculated perikaryonal vacuoles. **b** Solitary tract of a BSE-affected cow with marked neuropil vacuolation of the neuropil. Adjacent white matter tracts are unaffected. **c** Dorsal (parasympathetic) nucleus of vagal tract of a scrapie-affected sheep showing both neuronal perikaryonal vacuoles and neuropil vacuolation. **d** Dorsal (parasympathetic) nucleus of vagal tract sheep clinically sick with scrapie following experimental SSBP/1 challenge. Vacuoles are not evident by routine histology. **e** Diffuse grey matter vacuolation of the hippocampus and cerebrum in the ME7 scrapie strain. **f** Cerebellar molecular layer of a sheep with atypical scrapie. Vacuoles are smaller and more regular than in other classical forms of disease. All sections are stained with haematoxylin and eosin. **a** ×450; **b** ×160; **c** ×140; **d** ×140, **e** ×50; **f** ×140

that segregate according to experimental sheep [51], goat [81] and deer [116] passaged strains. Natural sources of scrapie in sheep, which behave as strains in the field, can be discriminated using the same methods [53].

Natural and experimental ruminant classical TSE strains show few differences in neuroanatomic targeting—as assessed by PrP^d accumulation—but major differences in cell-type targeting [53]. Other major strain-related variations are also found in the proportions of PrP^d processed intra-cellularly and extra-cellularly, and in the capacity of extra-cellular PrP^d to form amyloid fibrils and plaques [53]. In contrast, cloned murine strains show major differences in neuroanatomic targeting of PrP^d accumulation in different brain regions [17] (Fig. 3), but fewer changes in the cell-type targeting or processing of PrP^d.

Historically, some investigators suggested that murine scrapie strains existed in two forms that were defined by the *PRNP* genotype of the host: one strain was generated in the $PRNP^a$ genotype and one in the $PRNP^b$ genotype [23, 128]. Subsequently, numerous cloned strains have been defined in each mouse *PRNP* genotype [20]. More recently data has again been presented to suggest that sheep pathological phenotypes also segregate according to valine or alanine expression at codon 136 of the ovine *PRNP* gene [143]. However, such reports examined brain stem alone to characterise the disease phenotype, were from a restricted geographical area, and examined mainly homozygotes at that codon. When these data are examined critically, different within-genotype variations of PrP^d patterns are evident within single sheep genotypes. Other studies comparing natural scrapie sources across Europe confirm that different pathological phenotypes can be identified within sheep that are homozygous for alanine at codon 136 (González et al., submitted). Furthermore, when some experimental TSE strains are inoculated into sheep of different *PRNP* genotypes, the same pathological characteristics can be maintained [52, 115]. These data show that different pathological phenotypes of scrapie can be found in natural disease suggesting that there may be numerous naturally occurring sheep scrapie strains. In addition, at least under experimental circumstances, sheep adapted strains are not limited to particular *PRNP* genotypes.

In addition to different patterns of cellular affinity and processing of PrP^d, different aggregation and truncation states may also be recognised. PrP^d in the form of amyloid plaques as confirmed by tinctorial staining methods, finely punctate patterns (often referred to as 'synaptic') and truncated intracellular aggregates can be recognised by light microscopy. In the first of these forms, PrP^d is visibly aggregated into ~8–10 nm diameter filaments when viewed using the electron microscope while the other two are composed of PrP^d molecules that are not visibly aggregated. The proportions of fibrillar, non-fibrillar and intracellular forms of PrP^d differ in different diseases and strains. In cattle BSE plaques are absent [155], but small plaques are abundant in L-type BSE [25]. Intracellular PrP^d accumulation can occur in astrocytes, microglia and

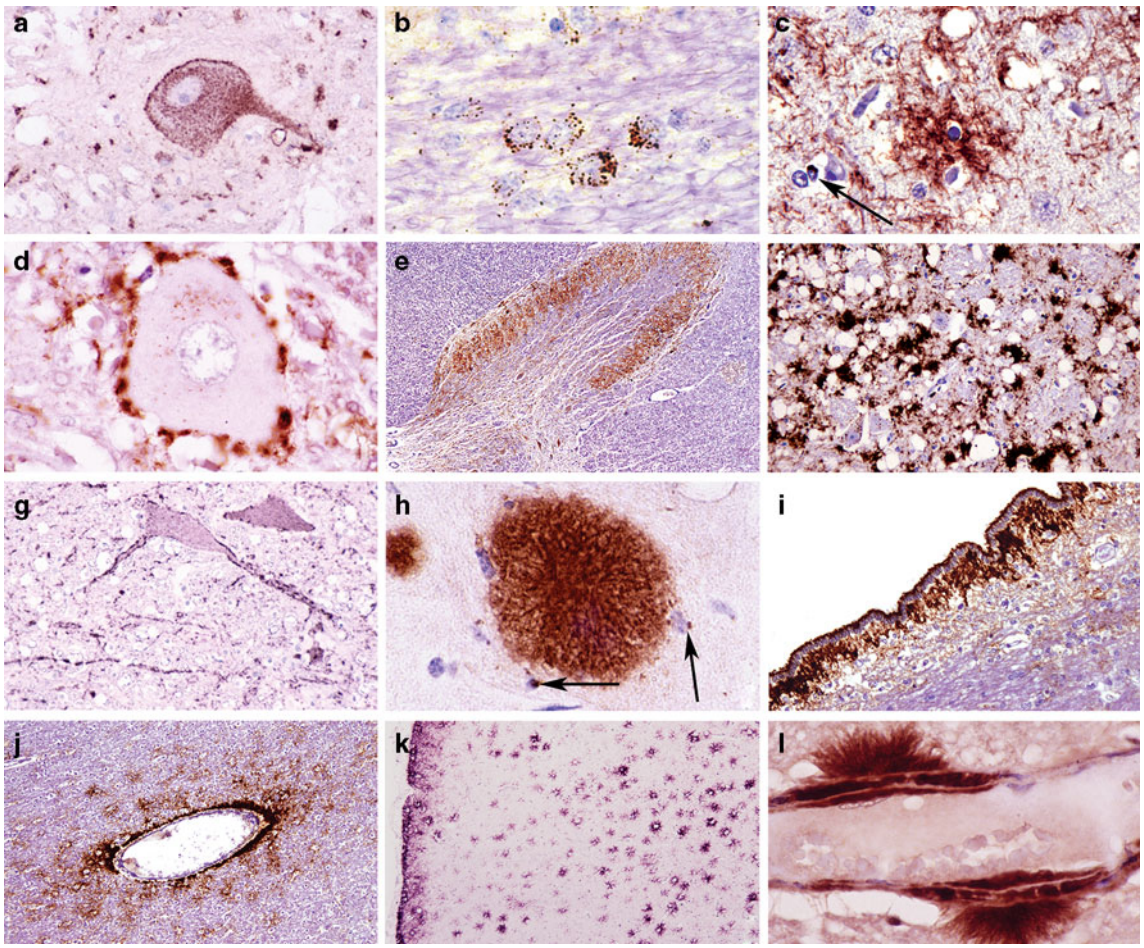

Fig. 2 Morphological types of PrP^d accumulation. There are a wide range of morphological forms of PrP^d accumulation associated with neurons, astrocytes, microglia and the ependyma: **a** FSE (cat), intra-neuronal **b** scrapie (sheep), intra-astrocytic **c** scrapie (sheep) stellate and intra-microglial (*arrow*), **d** BSE (cow) peri-neuronal, **e** scrapie (goat) diffuse punctuate, **f** CWD (white-tailed deer) coalescing, **g** FSE (Lion) linear, **h** 87V scrapie (mouse) plaque and intramicroglial (arrows), **i** scrapie (sheep) sub-ependymal and associated with luminal border of ependymal cells, **k** scrapie (sheep) sub-pial and stellate l) scrapie (sheep) vascular amyloid. **a** ×150, **b** ×600, **c** ×600, ×500, **e** ×50, **f** ×200, **g** ×150, **h** ×600, **i** ×150, **j** ×75, **k** ×75, **l** ×150

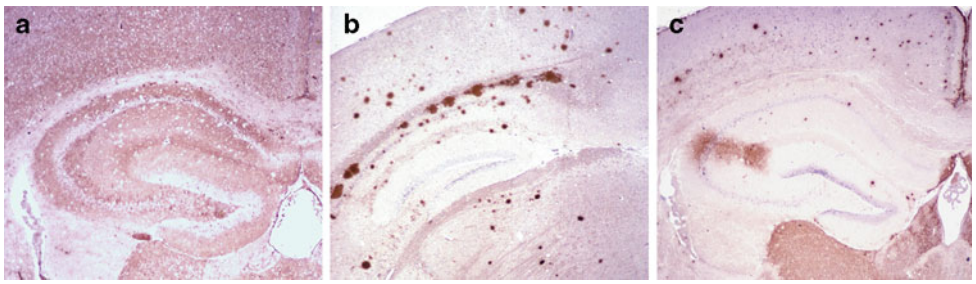

Fig. 3 Neuroanatomic targeting of PrP^d in mice: ruminant sources of scrapie show limited variability in neuroanatomic targeting as shown by PrP^d accumulation but significant variability in targeting is found in murine adapted scrapie strains. **a** ME7 scrapie showing diffuse PrP^d accumulation in cerebral cortex, hippocampus and thalamus. **b** 87V scrapie shows precise targeting to the CA2 sector of the hippocampus, plaques in the cerebral cortex and diffuse labelling in thalamus. **c** 111a is a prolific plaque-forming model, predominantly affected are the peri-ventricular and sub-pial locations. **a** ×30; **b** ×20; **c**) ×20

neurons as well as in macrophages of the lymphoid system. In each cell type it is largely present within lysosomes (see below). Non-intracellular PrP^d, including amyloid fibrils, are immunoreactive in situ with antibodies recognising either the N or the C termini of PrP [75], but intracellular PrP^d has markedly diminished immunoreactivity to

N-terminal PrP antibodies [80, 82]. The sub-cellular location and N-terminal degradation of intracellular PrP^d suggest that it is progressively degraded by the acidic environment and enzymes found in endo-lysosomes. The precise molecular site of intracellular truncation of the PrP^d molecule differs according to strain, but also to cell type. BSE-affected sheep have different intracellular truncation sites for neurons, glia and macrophages [80]. This is indirect evidence to suggest that different conformations of PrP^d can be derived from a single strain and has implications for the prion hypothesis as it indicates that not all conformational variants of PrP^d code for difference in strain properties.

The glycoform ratio of PrP^{res} and the mobility of its unglycosylated moiety as detected by Western blotting after partial protease digestion are often used to distinguish between strains, and is often referred to as the 'molecular strain type'. Immunoblots of PrP^{res} can be used to provide reliable presumptive strain characterisation for some species and strain combinations. Ovine BSE can generally be segregated from most naturally occurring classical scrapie sources by the mobility of the aglycosyl fragment though a small minority of naturally occurring sources [4, 145] and the CH1641 experimental sheep scrapie strain can only be distinguished from BSE by the glycoform ratios [61, 146] and transmission characteristics in mice. However, there are many sheep scrapie sources with distinct pathological characteristics that have identical PrP^{res} forms on Western blotting (González et al., submitted). As described above, immunohistochemistry shows that non-intracellular PrP^d accumulations are present as full-length forms in situ, whereas intracellular PrP^d is truncated. Thus, PrP^{res} obtained by Western blotting from brain homogenates treated with proteases represents a complex of original whole length protein derived from different cell types combined with truncated intracellular PrP^d types potentially of different fragment sizes. That different cell types may digest PrP^d at different sites in vivo indicates that extrapolations made from mobility of the protease-resistant fragment to strain need to be made with caution. A detailed discussion of the relationship between pathology, molecular strain typing or bioassay is beyond the scope of this review.

Accumulations of PrP^d (and also PrP^{res}) present in atypical ruminant prion diseases differ markedly from classical forms. Atypical (or Nor 98) scrapie is characterised mainly by a variable finely punctuate pattern of PrP^d accumulation in grey matter—most commonly in the cerebellum and cerebral cortices—and a fine punctuate pattern of PrP^d accumulation in white matter [11, 123] (Fig. 4). The so-called BASE strain or L-type cattle BSE is mainly characterised by diffuse distribution of plaques [25].

The nature and range of sub-cellular changes, their specificity for prion disease and co-localisation with PrP^d

Morphological changes and PrP^d: correlation between light and electron microscopy observations

Vacuolation, gliosis and neuronal loss are frequently found in brain regions where PrP^d accumulation is present, albeit in studies of the temporal progression of disease PrP^d accumulation precedes the onset of these morphological changes. In addition to these well-recognised light microscopic changes, there are a number of lesions found in prion disease-affected brains that are best appreciated or only evident by electron microscopy. Figure 5 shows the correlation between cellular and sub-cellular PrP^d accumulations and morphological changes viewed by electron microscopy. Those PrP^d accumulations that can be visualised as intracellular by light microscopy are associated with alterations of the endo-lysosomal system, while PrP^d accumulations that are not visibly intracellular at light microscopy are associated with lesions of membranes or changes consequent to the accumulation or aggregation of PrP^d within the extracellular space. However, there are a number of changes that do not co-locate with PrP^d.

Some electron microscopy lesions appear to be unique to TSEs while most changes—particularly at late stage disease—are common to many chronic neurodegenerative conditions. Table 1 lists a selection of morphological changes that have been found in all animal prion diseases so far examined and whether they are specific to TSEs and co-localise with PrP^d. Prion-specific lesions that co-localise with PrP^d mostly relate to membranes of neurons (Fig. 6) or glia, but two apparently unique prion lesions—spongiform change and tubulovesicular bodies (Fig. 7a)—do not co-localise with PrP^d (Table 1). Non-specific changes may nevertheless be important in disease pathogenesis, and those that co-localise with PrP^d mainly affect endo-lysosomes and changes that are due to the down-stream effects of PrP^d aggregation in the extracellular space. Some non-specific changes that do not co-localise with PrP^d are also listed in Table 1 and shown in Fig. 7.

Specificity of ultrastructural changes and their relation to PrP^d accumulation

Prion-specific lesions that co-localise with PrP^d A characteristic CNS change found in rodent [77], sheep [42, 83], cattle [40] and feline (unpublished observations) prion diseases, and which often accompanies membrane PrP^d accumulation, is a marked increase in sub-membrane coated vesicles and pits. The pits often have bizarre extended, twisted necks forming clefts and invaginations of

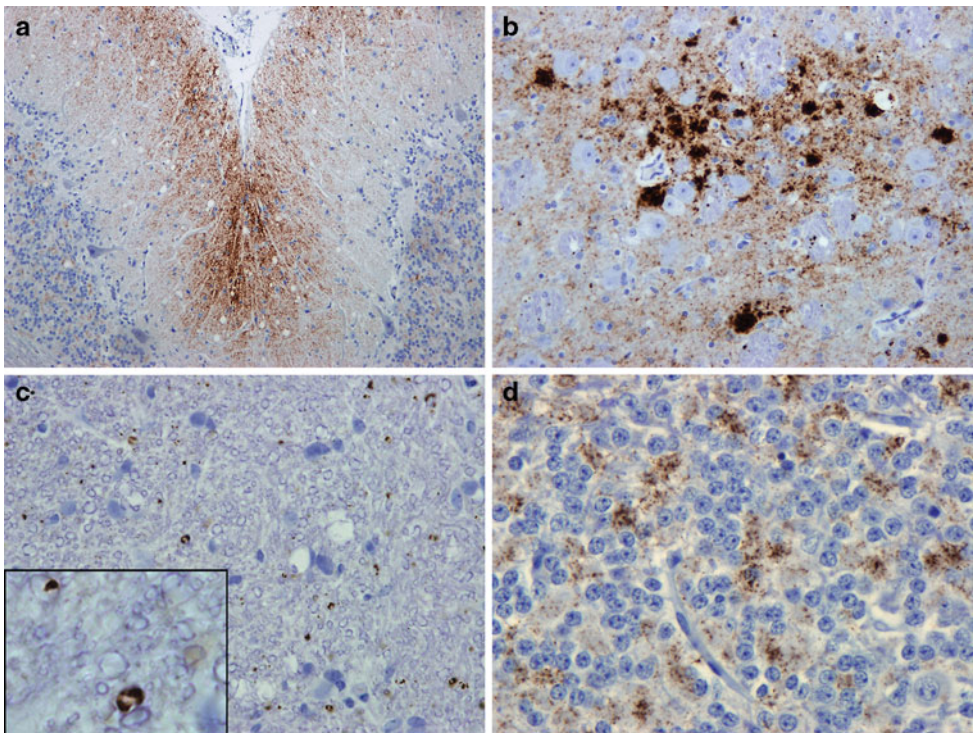

Fig. 4 Morphological types of PrP^d accumulation in atypical scrapie. Sheep and goats with atypical (or Nor 98) scrapie have patterns and neuroanatomical locations of PrP^d labelling that are distinct from the classical form of the disease. **a** Diffuse punctuate labelling of the cerebellar molecular layer. **b** Coarse punctuate PrP^d labelling of neuropil between granule cell neurons of the cerebellum. **c** Dense plaque-like deposits of PrP^d accumulation in the midbrain tectum. **d** White matter labelling of individual myelinated processes (inset shows PrP^d accumulation apparently within a myelinated axon). IHC for PrP^d labelling using L42 and F89 antibodies. **a** ×180; **b** ×450; **c** ×; **d** ×600 (inset ×1,000)

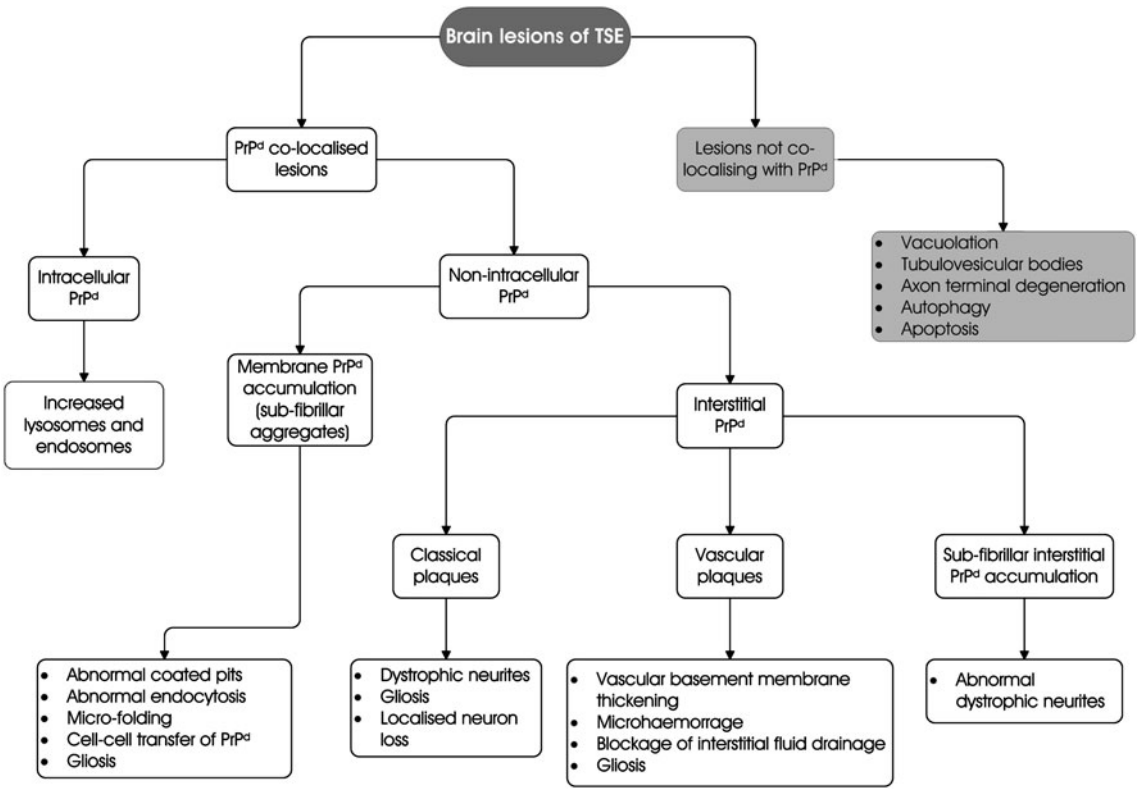

Fig. 5 Diagram showing the range of morphologic sub-cellular lesions found in TSEs and their correlation with presence, absence and cellular location of light microscopic PrP^d

Table 1 Consistency of selected sub-cellular lesions and their association with PrP^d labelling in classical animal TSEs and three murine transgenic systems

Lesion type: CNS			Species (strain)				Transgenic line (infecting strain)		
	TSE specific	PrPd +ve	Cat FSE[b]	Sheep scrapie	BSE	Mouse	Tg3*Prnp*$^{-/-}$ (RML)	Tg(PG14)	*TgGPI*$^{-/-}$ (RML)
Membrane clefts and coated pits in dendrites	**Yes**	**Yes**	**+**	**+**	**+**	**+**	+	−	−
Spiral coated structures in axonal boutons	**Yes**	**Yes**	**+**	**+**	**+**	**+**	+	−	−
Plasma-lemmal microfolds (glia and dendrites)	**Yes**	**Yes**	**+**	**+**	**+**	**+**	+	−	−
Irregular process contours	**Yes**	**Yes**	**+**	**+**	**+**	**+**	+	+	−
Neuronal perikaryonal cell membrane PrP^d	**Yes**	**Yes**	**+**	**+**	**+**	**+**	−	−	−
Dendrite plasma-lemmal PrP^d	**Yes**	**Yes**	**+**	**+**	**+**	**+**	+	+	−
Astrocyte plasma-lemmal PrP^d	**Yes**	**Yes**	**+**	**+**	**+**	**+**[a]	+	−	−
Axonal plasma membrane PrP^d	Yes	Yes	−	−	−	−	−	+	−
Vacuoles with membrane fragments	*Yes*	*No*	+	+	+	+	+	−	−
Tubulovesicular bodies	*Yes*	*No*	+	+	+	+	+	−	+
Excess glial lysosomes	No	Yes	+	+	+	+	+	−	−
Excess neuronal lysosomes	No	Yes	+	+	+	+	+	−	−
Individual extracellular amyloid fibrils	No	Yes	±	±	±	+	+	−	+
Amyloid plaques	No	Yes	−	+[a]	−	+[a]	−	−	+
Vasculopathy (basement membranes changes)	No	Yes	−	+[a]	−	−	−	−	+
Apoptosis	No	No	−	−	−	+	+	+	−
Degenerate terminal axons	No	No	−	−	−	+	+	−	−
Dystrophic neurites	No	No	+	+	+	+	+	+	+

+ Present, ± sparsely present, – absent. Bold represents a group of PrP^d positive membrane lesions that are common to all natural and experimental rodent TSE sources. Italics represent two lesions that are common to most natural and experimental TSE sources that do not co-localise with PrP^d

The TG3*Prnp*$^{-/-}$ mouse has neurons which lack capacity to generate PrP^c indicating that PrP^c expression on neurons is not mandatory for PrP^d-related membrane pathology [77]

The Tg(PG14) model [69] is a Gerstmann–Sträussler–Scheinker disease homologue that does not transmit disease [31] indicating that membrane PrP^d is not infectious

The TgGPI$^{\alpha-/-}$ is a model in which PrP^c is generated lacking its GPI anchor. This anchorless model confirms that the GPI anchor is necessary for membrane toxicity, but not for amyloid generation [28]

[a] Present in some strains or sources, but not in others

[b] Unpublished data on a single case

dendrite membranes. The coating on vesicles and pits resembles clathrin (Fig. 6), suggesting that PrP^d on cell membranes perturbs endocytosis by delaying or preventing excision of PrP^d-laden coated pits from the plasma membrane. Immunohistochemical studies have not shown any changes in the distribution of clathrin or the endocytosis-related proteins amphiphysin or dynamin, but ubiquitin co-localised with these membrane alterations (Fig. 6) [83].

PrP^c is attached to the exterior of the plasma membrane by its glycosyl-phosphatidyl-inositol (GPI) anchor. A large number of ligands are now known to interact with PrP^c and it has been implicated in a wide range of cellular functions (for review see [103]). So many potential roles and ligands for PrP^c have now been found that it has been suggested that PrP^c may act as a scaffolding protein in multiple sets of incompletely defined cell surface interactions and signalling mechanisms rather than have a specific interaction or function [103]. PrP^c cannot signal directly to cytoplasmic molecules from the exterior of the cell membrane, and it has long been assumed that endocytosis is mediated through a transmembrane signalling ligand [137]. Analysis of the distribution of immunogold particles suggests that PrP^d and ubiquitin are situated on the exterior and cytoplasmic faces of the membrane, respectively [83]. This suggests that PrP^d may also need a molecular partner to signal across the plasma membrane to ubiquitin and clathrin in order to initiate endocytosis (Fig. 8). When viewed by electron microscopy, the membrane located PrP^d is neither visibly aggregated nor it is associated with altered membrane dimensions. Why then is the PrP^d associated with excess coated vesicles and pits with extended necks? It is possible that PrP^d may be aggregated in two-dimensional sheets on the exterior of the plasma membrane aligned perpendicular to the axis of the clathrin-dependent mechanisms of

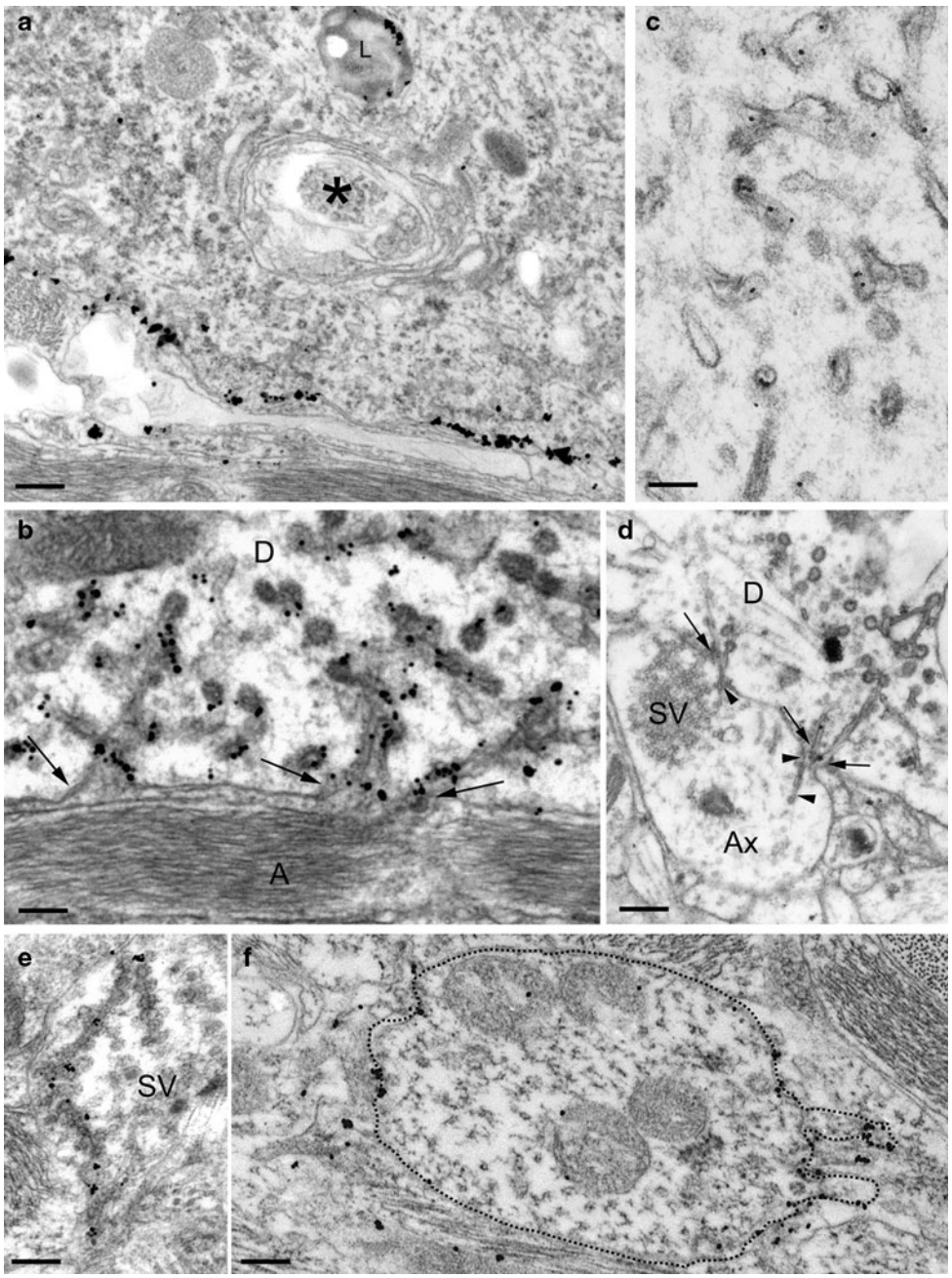

Fig. 6 Examples of scrapie and BSE-specific lesions that co-localise with PrP^d. **a** PrP^d accumulation may occur on a neuronal plasmalemma without morphological change. Weak PrP^d labelling is also present in a single lysosome (*L*), but not on a small autophagosome (*asterisk*). Sheep scrapie immunogold PrP^d labelling using R523.7 antibody. *Bar* 0.34 μm. **b** PrP^d accumulation in association with a dendrite shaft (*D*). Dendritic membrane invaginations (*arrows*) and coated vesicles are labelled for PrP^d. An astrocyte process is shown at A. Sheep scrapie immunogold PrP^d labelling using R523.7 antibody. *Bar* 0.15 μm. **c** Part of a dendrite showing abnormal invaginations and coated vesicles which are labelled for ubiquitin. Sheep scrapie immunogold ubiquitin labelling. *Bar* 0.17 μm. **d** A dendrite (*D*) shows numerous coated vesicles, some of which are connected via twisted membranes. At three points (*arrows*) on the dendrite twisted membranes are inverted from the plasma membrane. At a point immediately adjacent to the membrane invaginations of the dendrite are additional membrane invaginations (*open arrowheads*) on an axonal plasma membrane, identified by the presence of SV. *Bar* 0.32 μm. Cattle BSE uranyl acetate and lead citrate (not immunolabelled). **e** Inclusions within an axon terminal also consisting of a membrane invagination lined with vesicles. The coating of the membrane invagination consists of a lucent vesicular coating. These inclusions are more weakly labelled for PrP^d than are those on dendrites. Sheep scrapie immunogold PrP^d labelling using R523.7 antibody. *Bar* 0.19 μm. **f** The dendrite shown is immunolabelled for PrP^d at two poles. At one pole the PrP^d labelling is associated with polyp like membrane folds. This microfolding of membranes is much more florid on astrocytic processes. Sheep scrapie immunogold labelled for PrP^d using R523.7 antibody. *Bar* 0.18 μm. *SV* synaptic vesicles

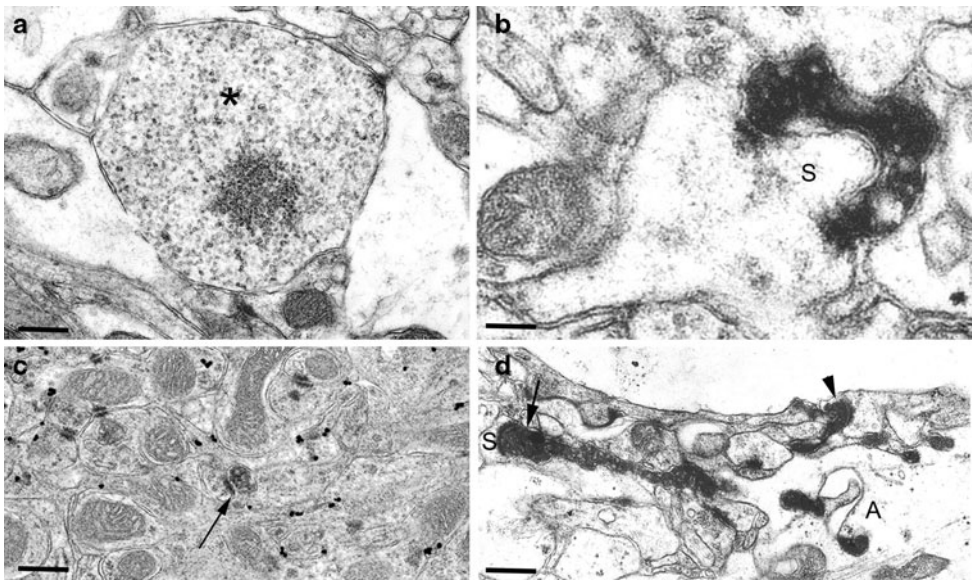

Fig. 7 Examples of scrapie-specific and non-specific lesions that do not precisely co-localise with PrP^d. **a** So-called tubulovesicular bodies (*asterisk*) from a mouse brain infected with ME7 scrapie. Some of the tubulovesicular particles form a paracrystalline array. They are not reactive with PrP^d by immunogold electron microscopy. Murine scrapie: immunogold PrP^d labelling using 1A8 antibody. *Bar* 0.26 μm. **b** Degenerate axon terminal (*asterisk*) which formerly synapsed with a complex dendritic spine characterised by a spinule (*s*). Murine scrapie. Uranyl acetate/lead citrate counter stain. *Bar* 15 nm. **c** Cerebellar molecular layer with PrP^d labelling of dendritic membranes. Degenerate axon terminals are non-labelled for PrP^d. Murine scrapie immunogold labelling for PrP^d using 1A8 antibody. *Bar* 0.41 μm. **d** Degenerate axon terminals (*arrowhead* and *arrow*) in the hippocampus of a mouse. One degenerate axon terminal is sectioned longitudinally and involves an extended length of the terminal axon, one end of which synapses with a spine (*s*) and the other is internalised by an astrocytic process (*A*). Murine scrapie: Uranyl acetate/lead citrate counter stain. *Bar* 0.40 μm

endocytosis, and that this may inhibit the efficient excision of pits containing PrP^d from the membrane. As a result, spiral twists in the elongated necks of coated pits may arise from torsional forces created by clathrin on 2D sheets of PrP^d aggregates on the membrane (Fig. 8d). Alternatively, as postulated for PrP^c, PrP^d may also act as a scaffold for many sets of cell surface ligands (Fig. 8e) (not excluding interaction with other PrP^c molecules), but in contrast to the scaffolds proposed with PrP^c, PrP^d may be too tightly bound or the complexes formed with other molecular partners may be too large for their efficient release from the membrane into endosomal vesicles.

The coated pits and vesicles beneath dendritic and somatic membranes may fuse to form complex branched cisterns (see Fig. 6c and also Fig. 9a in [83]) before merging with endo-lysosomes. Similar fused branched cisterns containing both PrP^d and ubiquitin are also present in macrophages of infected lymphoid tissues [118, 119]. However, macrophages internalise PrP^d from the exterior of the cell membrane by a non-coated endocytosis mechanism. These data suggest that membrane PrP^d may interact with different transmembrane ligands in different cell types supporting the idea that both PrP^c and PrP^d may have a multiplicity of cell membrane molecular interactors.

Amyloid may be deposited as a result of several different disease processes, but amyloid composed of PrP^d is specific to prion diseases. Amyloid fibrils present in both human and animal TSEs have been labelled by immunogold methods for PrP^d [35, 39, 71]. Unlike reports of amyloid accumulations of Gerstmann–Sträussler–Scheinker diseases [49], the amyloid fibrils within mature plaques found in murine and ovine scrapie strains, and also those of individual filaments found between cell processes, are labelled with both N- and C-terminal antibodies [75, 76]. Plaques appear to arise initially from focal accumulations of PrP^d on dendritic membranes, which can be released into the extracellular space [71]. Subsequent aggregation results first in formation of individual filaments irregularly located in the extracellular space between processes, leading ultimately to mature plaques composed of dense bundles of amyloid filaments surrounded by microglial cells [71]. Mature plaques, [142] and other extracellular PrP^d accumulations [117] also contain highly sulphated proteoglycans (as do plaques of Alzheimer's disease), which are present at early stages of disease progression. This suggests that extracellular matrix components may have a role in facilitating assembly of protofilaments. A transgenic mouse line, in which PrP^c lacks its membrane GPI anchor ($TgGPI^{-/-}$), has been generated [29]. Scrapie infection of $TgGPI^{-/-}$ mice results in abundant amyloid plaques that form initially within basement membranes of blood vessels [28]. Thus, amyloid plaques found in animal

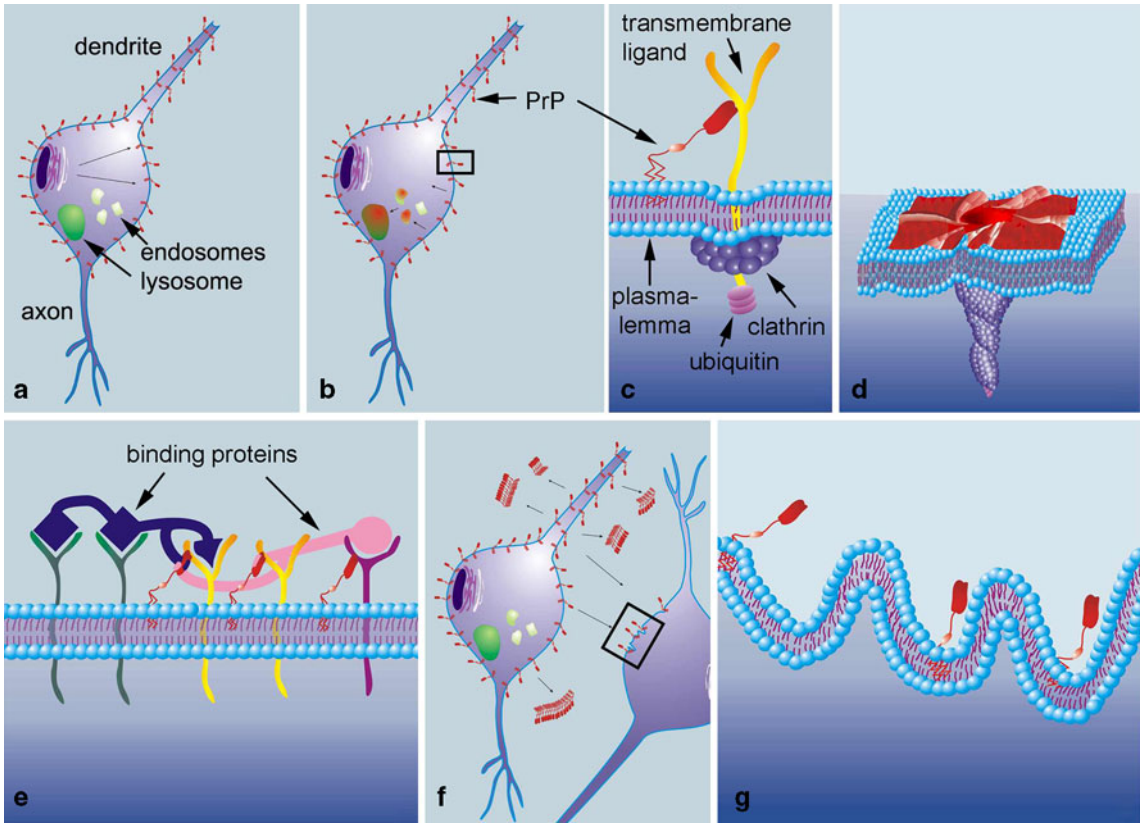

Fig. 8 Showing the proposed topology, membrane trafficking and pathology associated with PrP^d in classical forms of TSEs. **a** PrP^d is most commonly located on the plasma membrane. In contrast to PrP^c, which is generally localised to axons of mature neurons, PrP^d is found on perikaryonal and dendritic membranes. PrP^d at the cell surface may be retained, internalised or released. **b** PrP^d can be endocytosed to lysosomes where it is truncated. **c** PrP^d in clathrin coated vesicles and pits is associated with ubiquitin at the cytoplasmic face of the membrane. PrP^d putatively communicates to these cytoplasmic molecules via a membrane spanning ligand. The PrP^d-membrane spanning complex is inefficiently excised from the cell membrane for recycling or degradation. **d** and **e** show hypothetical arrangements in which PrP^d may inhibit efficient endocytosis. In **d** PrP^d isoforms are arranged in cross-linked two-dimensional sheets and in **e** PrP^d is shown forming stable multi-molecular complexes with other membrane proteins. **f** PrP^d on the cell membrane can be released probably involving cellular kinases and subsequently re-attach to adjacent membranes by its GPI anchor. Released PrP^d may also aggregate within the interstitial space (or basement membranes of blood vessels) to form amyloid fibrils. Fibrilisation is facilitated by interaction with interstitial molecules such as highly sulphated proteoglycans and the absence of GPI anchor. **g** PrP^d on membranes is also involved with complex membrane folding, particularly on glial cells. These pathways are not mutually exclusive and in sheep and cattle all pathways appears to be available for individual neurons

disease derive from full-length PrP^d released predominantly by dendrites into the extracellular space. The release of PrP^d to the extracellular space and subsequent aggregation into fibrils is facilitated by the absence of a GPI anchor and by interaction with unknown extracellular factors that may have a role in stabilising individual PrP^d molecules or protofilaments.

Marked irregularity of process contour profiles is another change found in dendrites and glial cells that also co-localises with intense PrP^d accumulation on plasma membranes. In severe cases, this change takes the form of microfolding of the membrane (Fig. 6) [40, 83]. Microfolding is particularly conspicuous on astrocytic membranes and is less often observed on dendritic membranes. Conversely, abnormal endocytosis commonly occurs where dendrites accumulate PrP^d at the cell membrane, but there is no evidence of abnormal endocytosis in the presence of membrane PrP^d on astrocytic or microglial membranes.

A coated spiral membrane structure is also found in axons and appears to be formed by spiral invagination of the plasma membrane (Fig. 6d, e). These spiral axonal membrane invaginations (originally called inclusions) have been recognised since some of the earliest electron microscopy studies, including those of human CJD [55], and originally were thought to be spiroplasma [6]. This feature is similar to the membrane invagination described in dendrites, but the membrane coating is not typical of clathrin and usually takes the form of empty vesicles of approximately 30–35 nm diameters (Fig. 6e). In addition, although this lesion also co-localises with PrP^d [40, 83] and ubiquitin, the amounts of immunogold reactivity for both of these proteins on axonal spiral membrane structures are

considerably less when compared with labelling of dendritic membrane invaginations (Fig. 6e). The axon plasma membranes surrounding these spiral membrane invaginations are not specifically labelled by PrP^d, but often arise immediately adjacent to dendritic invaginations (Fig. 6d) or dendritic membrane labelled PrP^d. This suggests that dendrite-derived PrP^d is the origin of the corresponding axonal change.

Prion-specific lesions that do not co-localise with PrP^d Vacuolation or spongy change is a common CNS response to a wide variety of toxic, metabolic and infectious diseases. The vacuoles or spongiform change found in scrapie-affected brains arise by at least two morphological routes: one form is associated with swelling of dendrites and axons and with a loss of intracellular organelles; a second form arises by dilation of membrane bound organelles within neurites and neuronal perikarya [2, 41, 84]. The first type of vacuole probably corresponds to dendritic varicosities that appear to be stable within dendrites over prolonged periods [47]. Some sub-cellular features of mainly larger vacuoles of uncertain primary morphogenesis do not appear to occur in other spongy degenerations and may be considered as prion-specific. Prion-specific vacuole features are mainly a peripheral fragmentation of the vacuole membrane combined with collapse of other neuropil components into a vacuolar lumen containing membrane and granular osmiophilic granules accompanied by apparent dissolution of these contents [2, 7, 84]. There is no PrP^d localisation to the contents or limiting membranes of vacuoles.

So-called tubulovesicular bodies (Fig. 7a) were first reported in scrapie-infected mouse brains as early as 1968 [34], but have not so far been described in other neurodegenerative diseases [100]. They have been detected in all animal TSEs so far examined, most consistently in mice and hamsters, and also in several variants of prion disease in man [96, 101]. They are oval or short tubular structures of approximately 35 nm diameter [3] that can be seen in thin sections arranged in clusters in dendrites or mixed with synaptic vesicles in axon terminals [96], but their biochemical and molecular structure remains unknown. A particle of similar dimension has been observed in a 120S fraction of brain homogenates centrifuged on sucrose buffers [112]. However, because of method differences it is not possible to know whether these individual structures are identical to tubulovesicular bodies seen by transmission electron microscopy.

Tubulovesicular bodies are only readily distinguished from other small ovoidal cytoplasmic structures when they occur in large clusters, which may explain why they are not always observed in brains of individual prion disease-affected animals. In two series of BSE-affected cattle or scrapie-affected sheep, tubulovesicular bodies were seen only in 1 of 10 cows [40] and 2 of 10 sheep examined [41]. Tubulovesicular bodies have not been observed outside the CNS, or in infected tissue culture, nor have they been detected in the Tg(Pg14) mouse (Table 1), a non-infectious transgenic model of a Gerstmann–Sträussler–Scheinker disorder [69]. In two separate studies of rodent scrapie, tubulovesicular bodies were detected at early stages of infection prior to the onset of other neurodegenerative changes [65, 102], which suggests that they are not a non-specific sequel to other aspects of scrapie degenerative changes. Ultrastructural immunogold detection methods do not show co-localisation of tubulovesicular bodies with PrP^d [68, 98].

Prion non-specific lesions that co-localise with PrP^d In agreement with observations of human CJD [91], several animal studies have suggested that lysosomes and/or multivesicular bodies (late endosomes) may be increased in sheep scrapie [43] and cattle BSE [40]. These semi-quantitative evaluations are supported by evidence that ubiquitin (of presumptive lysosomal origin) is increased from approximately 20% of incubation period in murine scrapie [105] and that lysosomal cathepsins are implicated in the degradation of PrP^d in scrapie-infected cultured cells [106]. In a recent study, the number and size of lysosomes in neuronal perikarya were shown to be increased in sheep scrapie [83]. Many morphologically normal and some enlarged or irregularly contoured lysosomes are labelled for PrP^d by immunogold methods. As mentioned above, light microscopic studies show that intracellular PrP^d lacks immunoreactivity to N-terminal PrP antibodies [80]. Together these data suggest that internalised PrP^d is targeted to lysosomes for degradation.

Prion non-specific lesions that do not co-localise with PrP^d As is usual for chronic neurodegenerative disease, there is a wide spectrum of lesions that have been described in TSE-affected brains. Neuronal apoptosis, autophagy, axon terminal degeneration, dystrophic neurites, gliosis, dendritic varicosities, synaptic vesicle clumping and losses of synapses and dendritic spines are just a few of the more important lesions. To date no specific localisation of PrP^d to any of the above changes is reported.

Qualitative and quantitative variability of cellular and sub-cellular changes

Variability observed between different TSEs in different species

The characteristics of infectious disease are the result of an interaction between strain properties and the genetics of the

host. Because the key informational determinants of a prion strain are undefined, strains are characterised by their disease phenotype, principally their clinical, pathological and biochemical properties. It is therefore often difficult to know whether changes in disease phenotype on passage to a new host are caused by differences between host and recipient genetics, or following adaptation or mutation of the strain on passage to the new host. This is particularly the case when a strain is passed to another species. However, when several different rodent prion strains are compared with disease in ruminants, some features of rodent prion diseases are consistently different from those of classical prion diseases of ruminants.

In addition to the neuroanatomic and cellular targeting differences seen when rodent scrapie strains are compared with ruminant strains and sources (see "The nature and range of neuropathological changes"), a selective terminal axon degeneration is conspicuous in mice and has been seen following challenge with several cloned scrapie strains [78, 138] (Fig. 7). It also occurs in a scrapie-infected transgenic model in which PrP^{c} expression was confined to astrocytes while lacking on neurons [77, 131] indicating that this change is not a "loss of PrP^{c} function" effect. Axon terminal degeneration may be temporally coincident with morphometrically determined synaptic loss at very early stages of disease (see below), but is absent from cats, cattle and sheep (Table 1). Similarly, apoptosis can be frequent in some rodent scrapie strains, but is rare or absent in sheep and cattle TSEs.

Classical amyloid plaques or kuru plaques are relatively infrequent except in some specific strains, such as the 87V [17] or 111a [76] strains or in the scrapie-infected $TgGPI^{-/-}$ transgenic line [29]. However, amyloid, in the form of single randomly orientated short fibrils within the extracellular space, is frequently present in other rodent scrapie strains [73]. In contrast, amyloid, either in the form of individual fibrils detectable in the electron microscope or plaques visible by tinctorial staining methods at light microscopy, is absent in the neuropil of most classical ruminant prion diseases, albeit it may be an important feature of L-type BSE, one of the atypical prion diseases of cattle. This may suggest that PrP^{d} is released much more readily from the surface of rodent cells than it is from the surface of ruminant TSE-infected cells.

Thus, three differences may be recognised when cloned murine scrapie strains are compared with natural sheep scrapie and cattle BSE, and might represent species-specific responses to classical TSEs. There are significant differences in cell tropisms, in the processing and release of PrP^{d} from infected cells and in clinically significant axon terminal and synapse degenerations. We surmise that the mouse may preferentially select for only some features of prion infection that occur in the original donors. While what is learnt from any single murine strain will always be helpful in the understanding of disease pathogenesis, the study of disease in natural hosts remains essential.

Variability attributable to TSE strain and/or host PRNP genotype

As described earlier, significant differences in patterns of PrP^{d} accumulation have been found for different classical mouse, sheep, goat and deer TSE strains and sources, yet, where examined at the ultrastructural level, specific membrane changes are present in each of them. The features described above (membrane PrP^{d} accumulation, membranes with excess coated pits and invaginations, membrane microfolding) have all been identified in mice, cattle, sheep and cats (Table 1). There is no meaningful data on the effect of strain on sub-cellular pathology for many of these changes, but in sheep scrapie the frequency of all of the above varied according to source and partially to *PRNP* genotype [40, 83] suggesting that the processing of membrane PrP^{d} is influenced by strain and/or *PRNP* gene factors.

Amyloid plaques composed of PrP^{d} and forming within blood vessels (cerebral amyloid angiopathy) of TSE-affected animal brains have a pathogenesis that is similar to cerebral amyloid angiopathy of Alzheimer's disease. Vascular plaques initially form within basement membranes of endothelium and smooth muscle and consequently obstruct CNS interstitial fluid drainage pathways [28]. Cerebrovascular plaques are common in some natural sources or strains of scrapie [53] and occur in chronic wasting disease-affected deer [97], but are absent from cattle BSE. A model of scrapie derived from chronic wasting disease, the 409V model [19] also produces abundant cerebrovascular plaques. As described above, cerebrovascular amyloid is also particularly abundant in scrapie-infected transgenic mice ($TgGPI^{-/-}$) expressing PrP^{c} that lacks the GPI membrane anchor [29] as do some rare human Gerstmann–Sträussler–Scheinker variants [132] which also lack anchored forms of PrP^{c}. Anchorless PrP^{res} is found as a subset of the range of PrP^{res} forms produced in classical prion disease [147]. It is possible that some naturally occurring prion strains may produce higher proportions of anchorless PrP^{res} or anchorless PrP^{d} than others. Thus, the proportions of different molecular variants of PrP^{d} present in particular strains may influence the nature of the histological, cellular and sub-cellular pathology.

Processing of PrP^{d} in the brain

PrP^{d} may accumulate on membranes, be endocytosed from the plasma membrane, be transferred between cells, or be released into the extracellular space.

Discrepancies in membrane localisation of PrP^c and PrP^d

PrP^c is transported in vitro along secretory, endocytic and axonal transport pathways to the cell membrane [60]. Both retrograde (to soma) [124] and fast anterograde (from soma) [133] transport of PrP^c is reported and it has been localised to the surface of retinal explanted axons [135] and cell bodies of ganglion neurons [109]. At early stages of development, PrP^c was found on membranes of all hippocampal neurites, but in the mature hippocampus, PrP^c was selectively partitioned into detergent-resistant cholesterol-sphingolipid rich domains on axons [48]. It seems likely that the C terminal GPI anchor and flexible N terminus of PrP^c are both necessary for its correct trafficking and distribution [153] to detergent-resistant domains on mature axons. Studies of PrP^c localisation in vivo have produced contradictory results. Several studies support in vitro data that indicates PrP^c passes through the Golgi apparatus before being transported to neuronal membranes with a distribution that favours axons at the expense of dendrites, and is recycled via multivesicular bodies (a late endosome) [92, 122]. Membrane PrP^c on axons excludes the active zones of the synapse and the post-synaptic density of the corresponding dendrites, and is also found on astrocytic membranes [92]. In contrast, other studies have detected PrP^c in association with synaptic vesicles, but not plasma-lemmas [59, 125]. Unknown technical reasons may account for these different results.

Original pulse chase experiments proposed that conversion of PrP^c to its disease-specific counterpart occurred at the plasma-lemma or at some later stage in the cell cycle [27]. In vivo observations of sub-cellular PrP^d localisation of prion-infected mice [73], sheep [83] and cattle [40] show that it is most frequently and abundantly found on morphologically normal membranes of dendrites, neuronal perikarya and the processes of astrocytes, further suggesting cell membranes are the primary site of accumulation and the transformation of PrP^c to PrP^d. Recently, a similar conclusion was reached using immunogold to localise PrP^c and PrP^d in vitro in scrapie-infected N_2A cells [151]. The diffuse punctuate labelling that is often referred to as 'synaptic type' on examination at light microscopy is found at electron microscopy to label predominantly dendritic membranes [40, 50, 70, 83] and not axons. Dendritic and somatic membrane PrP^d accumulations of neurons are found in all classical forms of animal prion diseases examined (Table 1). Unmyelinated axons, terminal segments of myelinated axons and the active zone of the pre-synaptic bouton or post-synaptic densities of the CNS are not specifically labelled for PrP^d in the classical TSEs. That PrP^c is converted to PrP^d predominantly on dendritic and somatic membranes and not on axons in all the classical animal prion diseases indicates either that cell membrane PrP^c trafficking is perturbed during scrapie infection or that the conditions for conversion of PrP^c to PrP^d are more favourable on dendrites and perikarya than on axons.

Although most PrP^d in classical TSEs is found in association with dendrites and soma, axonal PrP^d has been inferred or demonstrated in the peripheral nervous system. PrP^d labelling of peripheral nerve axons has been observed by light microscopy in felids [94], BSE-infected cattle and scrapie-infected sheep [58]. Although the sub-cellular localisation of this PrP^d is not established, data from several sources suggest that this is anterogradely transported PrP^d from neuronal soma in the CNS. Atypical scrapie also shows significant labelling of CNS white matter tracts at light microscopy (Fig. 4) [123] and preliminary data suggest that this PrP^d is at least partly within axons (Jeffrey and Moore, unpublished observations). Both intra-axonal [120] and axonal plasma membrane labelling of unmyelinated CNS axons is present in the Tg(PG14) mouse, a transgenic non-infectious rodent model of a Gerstmann–Sträussler–Scheinker disorder [69]. This model shows a number of unique pathology features, which probably relate to the transgenic manipulation. These data suggest that the trafficking of PrP^d may differ in the central and peripheral nervous systems, and may also be influenced by atypical sources and *PRNP* genetics.

Accumulation on the plasma membrane

PrP^d molecules revealed by immunogold methods at the cell surface are not visibly aggregated when viewed by transmission electron microscopy. Given the resolution of the electron microscope, PrP^d localised by immunogold methods cannot be accurately resolved to monomeric, dimeric or oligomeric forms. Depending on the energy of the electron beam and the thickness of the section, it is probably not possible to detect PrP^d in aggregates of less than 6–15 molecules. Plasma membranes are 7–8 nm thick and are composed of three layers each approximately 2.5–3 nm thick. As the thickness and structure of plasma membranes containing PrP^d are not visibly changed, this suggests that the PrP^d on membranes may not initially be arranged in large amorphous, globular or fibrillar aggregates. Similarly, the molecular impacts of PrP^d accumulation on the cell membrane are not certain. In vitro studies have shown that recombinant PrP folded into predominantly alpha or beta forms has different interactions with membrane lipids [87] while most cells that accumulate PrP^d on the cell membrane generally do not show morphological changes.

Endocytosis

As described above, cell membrane-attached PrP^d is associated with morphological evidence of abnormal endocytosis.

This abnormal endocytosis is putatively elicited via a transmembrane ligand and associated with impaired excision from the cell membrane. In the lymphoreticular system, PrP^d accumulations in macrophages are also associated with abnormal endocytosis and sub-membrane ubiquitin accumulation, also suggesting linkage via a transmembrane ligand [119]. However, in macrophages, the endocytosis is via a non-classical pathway and PrP^d accumulation on follicular dendritic cells is associated with excess and abnormal cell-surface immunoglobulin trapping, suggesting additional PrP^d-membrane receptor interactions [119]. Thus, cell membrane PrP^d in lymphoid tissues would also appear to interact with receptors and ligands in membranes, but these molecular partners appear to be different from those in neurons. Cell membrane and lysosomal PrP^d accumulations occur in astrocytes, but endocytosis in glial cells does not appear to involve delayed excision of PrP^d from the cell membrane. These data suggest that endocytosis of PrP^d involves interaction with different ligands on different cells.

Transfer between cells

Studies of scrapie-infected cells have shown that exosomes can transfer infectivity to the culture medium and to other contiguous cells in culture [44, 152]. However, serial reconstructions of scrapie-infected neurons visualised by electron microscopy were not able to identify exosomes, which are 50–90 nm in diameter, on membranes or in the tissue spaces between infected neuronal perikarya and adjacent PrP^d positive cell processes [83]. Tunnelling nanotubes [26] have also been suggested as a mechanism by which infectivity may be transferred between cells in vitro, but they too have not so far been seen in vivo.

The interstitial space, or specifically the distances between neurites and or glial plasma-lemmas in mature brains, is usually of the order of 10–20 nm. Across these distances, GPI anchored proteins [63], including PrP^c [104] may be transferred by a process sometimes called GPI painting. When statistical approaches are applied, immunogold localisations of membrane PrP^d are shown to be located to the external parts of the membrane [83], a site that is consistent with its retention in the membrane by a GPI anchor. PrP^d can also be transferred between membranes. The evidence for this includes immunogold studies of sheep and murine scrapie and cattle BSE that visualise PrP^d on membranes immediately adjacent to scrapie-infected dendrites and neuronal perikarya. Additionally, in scrapie-infected Tg3$PRN^{-/-}$ mice where PrP^c is only produced by astrocytes, PrP^d was visualised on neuronal membranes adjacent to PrP^d-releasing astrocytes [77]. Intercellular transfer of GPI-anchored proteins is a regulated process that involves cellular activation by protein kinases [104]. This in turn suggests that membrane located PrP^d requires a transmembrane signalling partner to facilitate cellular activation and its transfer from one membrane to another.

Accumulation in the extracellular (interstitial) space

Some diffusible, probably soluble, PrP^d isoforms may be released by infected cells into the extracellular space where they may migrate away from their points of release through the interstitial space. PrP^d lacking a GPI anchor conspicuously follows intra-cranial interstitial fluid drainage pathways to exit the brain [28]. However, PrP^d/PrP^{res} does not appear to reach extra-cranial interstitial fluid drainage pathways and the cerebrospinal fluid in any significant amounts.

In Alzheimer's disease the formation of amyloid fibrils is promoted by concentration of Aß fragments, by pH and by extracellular factors [154]. PrP^d accumulations are also associated with alterations of the extracellular matrix and in particular with the loss of perineuronal nets [10], as well as with other more widely dispersed interactions with extracellular matrix components, such as sulphated proteoglycans [117]. The immobilisation of diffusible forms of PrP^d is likely facilitated by interaction with extracellular matrix components. PrP^d released in classical prion diseases may not leave the brain, but become fixed in situ. The absence of a GPI anchor facilitates initial amyloid formation within vascular basement membranes [28], but the reasons why amyloid plaques form where they do within the neuropil, or why some murine models have widely dispersed individual amyloid fibrils rather than classical plaques is still unclear.

Molecular interactions of PrP^c and PrP^d

As described above, the precise function or functions of PrP^c are unknown, but the extensive and diverse pathways now implicated suggest that PrP^c may serve as a scaffolding protein in multiple sets of cell membrane interactions with transmembrane ligands including those necessary for endocytosis of PrP^c molecules anchored to the outside of the plasma-lemma [137] (Fig. 8). Cell biology studies have suggested several molecules that may interact with PrP^d, and the morphometric and immunochemical data described above provide further indirect evidence for interactions with: a kinase partner to facilitate an activated cell membrane transfer of PrP^d, a ligand participating in abnormal clathrin-mediated endocytosis in neurons, and a ligand participating in abnormal non-clathrin-mediated endocytosis in macrophages, also suggesting that PrP^d may act as a scaffold for several membrane partners.

Given the potential functions of PrP^c and the inference that PrP^d may also act as a scaffolding molecule, we suggest that monomers or small aggregates of PrP^d may link

irreversibly with other membrane proteins—possibly those with which PrP^c also interacts—to form stable PrP^d-protein complexes. These more stable complexes may be formed by increased affinity of monomeric PrP^d for other membrane molecules or by cross-linked 2D sheets of PrP^d with other PrP^d molecules (Fig. 8). Endocytosis mechanisms may find it difficult to efficiently internalise PrP^d from these stable complexes for lysosomal degradation, albeit abundant lysosomal PrP^d indicates that significant fractions of PrP^d do eventually reach lysosomes. Facilitators or inhibitors of PrP^d endocytosis could also include components of the extracellular matrix.

Correlation between pathological changes and clinical disease

Morphological changes and disease: nature and distribution of lesions in relation to clinical signs

Classical descriptions of prion diseases cite vacuolation, gliosis and neuronal loss as the predominant lesions of most animal prion diseases yet none of these features is consistently present when different animal diseases and strains are considered. Although vacuolation is prominent in most field cases of disease, it is virtually absent in clinically sick mink of the Chediak–Higashi genotype [114], or in sheep experimentally infected with the SSBP/1 strain of classical scrapie (Fig. 1) [8]. Though formal data are limited, immunohistochemical or morphologic assessments of gliosis does not suggest an early or primary role of gliosis in disease [108, 155]. Many molecular and cell biology studies presume that clinical disease is linked to apoptotic neuronal loss, a supposition that is supported by several lines of investigation [90]. In large animals, an increase in pro-apoptotic factors, such as Bax expression has been reported in sheep scrapie [136] and morphometric studies have shown neuronal loss in some BSE cattle brain stem sites [79]. However, techniques, such as TUNEL or other immunological methods have not been able to show that apoptotic neuron loss or the expression of pro-apoptotic markers occurs in significant numbers either in cattle BSE [149] or sheep scrapie [107]. Furthermore, in BSE-affected cattle neuronal numbers at several key anatomic nuclei are not significantly different from controls [79]. Where neuronal loss is unambiguously present in rodent models it is not reversed by studies which prevent neuronal degeneration [148], nor does it occur sufficiently early to explain clinical disease onset [33, 66]. Thus, while neuronal loss and apoptosis may contribute to some clinical disease signs in some diseases, it is only present at late stages and cannot be causally linked with clinical onset or clinical disease progression.

In contrast, synaptic [78] and spine loss [16] has been demonstrated at early stages of rodent disease where it has been shown to correlate with the earliest behavioural changes [33]. The synaptic unit consists of the axonal pre-synaptic bouton including the active zone, the synaptic cleft and the post-synaptic (usually) dendritic contact. Synaptic loss has been closely studied in the *stratum radiatum* of the hippocampus where losses start at about 34% of the incubation period of ME7 rodent scrapie [78]. In the same model, dendritic spines are also progressively lost from early stages of disease [9, 16]. In vivo imaging shows that only permanent spines are lost and transient spines maintained suggesting an ongoing attempted compensatory response [47]. Similarly, an increase in the size of synapses, also considered compensatory, has also been observed in murine scrapie [138]. Several studies of rodent scrapie have provided data suggesting that degeneration may be initiated in the pre-synaptic terminal axon. First, degeneration of synaptic structures is not confined to the synaptic bouton, but involves segments of the terminal axon (Fig. 7d) [78]. Second, detectable dendritic spine loss is recognised at 108 days [16] in a model where synapse loss starts about 20–30 days earlier [56, 78]. Third, intact spines without axon contacts increase through the incubation period [56], and fourth, the loss of synaptic integrity is accompanied by diminished protein expression associated with synaptic vesicles, synaptic membranes, synaptic adhesion, neurotransmitter release and post-synaptic structures on dendritic spines [1, 56, 66, 141]. Most of these changes of protein expression have been recognised after morphologic and morphometric evidence of synaptic and spine loss, but the loss of pre-synaptic proteins is generally more extensive than the loss of post-synaptic proteins [56]. Together, these data suggest that degeneration is initiated in the pre-synaptic terminal axon.

In murine ME7 scrapie PrP^d accumulation begins in the dentate gyrus rather than in the *stratum radiatum* and neither the magnitude nor the spatial pattern of PrP^d accumulation correlates with number of synapses lost [56, 78]. Isolated synaptosomal fractions from scrapie-infected hamsters show abundant PrP^{res} by Western blotting [13], but such studies cannot be used to provide evidence of a relationship between PrP^d and synapse loss as synaptosomal fractions contain abundant dendritic spines (see Fig. 4 in [13]) and do not take into account the possibility that extracellular PrP^d derives from non-synaptic sources. When immunogold studies are used to localise PrP^d in vivo, it does not co-locate on degenerate axon terminals (Fig. 7d and [72]). Of particular interest is the Tg3/$Prnp^{-/-}$ mouse, in which axon terminal degeneration is found [77] even though neurons in this mouse do not express PrP^c, and PrP^d is generated solely by astrocytes [131]. Thus, the

deposition of PrP^d cannot be directly linked to axon terminal degeneration and synaptic loss.

In the hippocampus of ME7-infected mice, axon terminal degeneration is associated with predominantly asymmetric, excitatory and glutamatergic synapses. Lost synapses include both simple (Fig. 7a) and complex ones (Fig. 7b), putatively weak and re-enforced synapses, respectively [78]. As *N*-methyl-D-aspartic acid (NMDA) are common receptor types of excitatory transmission in the hippocampus, it is highly likely that these synapses are lost, but electrophysiological studies do not support a specific disturbance of NMDA or calcium channels in this model [86]. Terminal axon degeneration is not confined to ME7 mouse scrapie, but can be found in other murine strains and at other brain sites [77, 138]. In contrast, inhibitory *gamma*-aminobutyric acid (GABA) neurons and both GABA and non-GABA synapses are lost in the thalamus and cerebral cortex of scrapie-infected hamsters [13]. Sheep with natural scrapie show reduced numbers of the GABAergic neuronal subpopulation in cerebrum, striatum and thalamus. This neuronal loss is associated with reduced metabotropic glutamatergic receptor type I ($mGluR_1$) signalling in the striatum, thalamus and obex and up-regulation of protective adenosine receptors (A_1R) signals in the striatum (Sisó et al., submitted). These findings are in agreement with previous observations in human CJD and in murine models of BSE [134]. We infer from these data that the process of degeneration is not specific to a single class of axon terminals or their corresponding receptor subtypes, but may relate to a less specific perturbation of terminal axon function not necessarily confined to boutons.

Morphologic evidence of axon terminal degeneration is absent from cattle BSE or sheep scrapie. However, this does not rule out the possibility that the same molecular mechanisms underpinning synapse dysfunction in rodents may also occur in these species, but that they respond with a different morphological response or none. Synaptic autophagy is reported in human biopsy material [95] and is also found in cattle BSE and sheep scrapie (M Jeffrey, unpublished observations). Synapses containing aggregated synaptic vesicles are present in excess in hamster scrapie [13]. This feature also occurs in prion-diseased ruminants, although it is common in control tissues and its frequency is affected by technical issues. Dysfunction at the synapse or terminal axon levels remains the most likely proximate cause of neurological signs in prion disease, but the molecular causes remain entirely unclear.

PrP^d accumulation and disease: gain/loss of function

There are two proposals by which PrP^d may be considered to cause disease: an acquired toxicity (or the gain of function proposal) caused by accumulation of PrP^d forms, or a loss or subversion of normal PrP^c function caused either by removal of PrP^c or interference between PrP^d and PrP^c (reviewed in [103]). Experiments can be cited in support of each hypothesis, for example, there are numerous experiments that demonstrate that fibrillar PrP^{res} aggregates are toxic to cells in vitro [46], and several mechanisms have been shown whereby this toxicity may be manifested [90]. Conversely, elegant experiments have shown that when the expression of PrP^c in neurons is switched off in scrapie-infected conditional knockout mouse, a marked improvement in clinical signs immediately ensues and end-stage disease is delayed [110]. Similarly, when scrapie-infected mice are transfected with a PrP^c interfering RNA, disease is delayed [156]. These and other data have been interpreted to suggest that clinical signs are caused by a loss or subversion of PrP^c function.

A direct association between PrP^d accumulations on abnormal membrane structures involving an altered endocytotic process is found in all animal TSEs (Table 1) and indicates that membrane PrP^d accumulations can be associated with a toxic gain of function. Where extracellular PrP^d accumulates in excess, particularly where PrP^d forms fibrils and amyloid aggregates, other morphological changes comprising gliosis and neuronal dystrophia occur. These data indirectly suggest that fibrillar PrP^d may have additional toxic effects. Morphological changes, such as vacuolation and tubulovesicular bodies do not co-locate with PrP^d (Table 1; Figs. 5, 7a) and potentially represent changes that may be ascribed to a loss or subversion of PrP^c function. However, changes, such as vacuoles, tubulovesicular bodies and excess pits and abnormal membrane invaginations are all found in the neurons of scrapie-infected TG3$Prnp^{-/-}$ mice [77] which lack neuronal PrP^c expression [131]. It is therefore unlikely that these lesions are a direct result of subversion or loss of function of PrP^c.

Irrespective of possible mechanisms of toxicity, it has been known for many years that TSEs can be transmitted in the absence of detectable PrP^d or PrP^{res} [45, 93], and that such infectivity may be at modest or even high titres [5, 130]. Most recently, the converse situation has been encountered and PrP^d and amyloid plaques have been found in the absence of detectable infectivity [127]. In ruminant prion diseases, there are many, albeit less extreme, examples where the relationship between PrP^d accumulation and clinical disease breaks down. The following three examples are given here: BSE is a highly stable disease strain in ruminants that can be transmitted to sheep of different *PRNP* genotypes and by different routes of challenge. Though incubation periods are affected by *PRNP* genotype and route, the pathological and molecular features of the disease are not. When PrP^d profiling methods were used to quantify the abundance and distribution of PrP^d in different brain areas, the magnitude of

PrP^d accumulation bore no relation to incubation period [52]. Second, as discussed earlier, sheep with scrapie accumulate many different morphological forms of PrP^d some of which are intracytoplasmic forms in neurons and glia and others are membrane associated and extracellular forms [83]. Some sheep scrapie strains, exemplified by CH1641, accumulate almost exclusively intracellular forms of PrP^d while others, such as a highly studied natural Suffolk breed source, have almost exclusively membrane and extracellular forms [53, 67]. Thus, if disease is related to intracellular forms of PrP^d, then the natural source Suffolk sheep should not develop disease or, conversely if disease is related to extracellular forms of PrP^d then CH1641 sheep should not develop disease. Third, individual animals experimentally challenged with scrapie or BSE have developed clinical signs of TSE disease in the absence of pathology [89].

To address the conflict between PrP^d and/or PrP^{res} detection, clinical disease and infectivity, it has been suggested that most detected forms of PrP^d/PrP^{res} are not infectious while only some forms are disease causing [129]. The Tg(PG14) mouse, which develops a spontaneous disease and mimics a human form of Gerstmann–Sträussler–Scheinker disorder that has an octapeptide repeat insertional mutation, develops an ataxic disease phenotype, accumulates PrP^d in association with apoptotic neuronal loss, but the disease is not transmissible [30]. Thus, the Tg(PG14) mouse establishes the principle that a disease associated with accumulation of PrP^d may occur in the absence of infectivity. However, the pathology of this Tg(PG14) mouse is not altogether typical of classical forms of scrapie and prion disease (Table 1) [69] and, in order to accommodate the discordances between PrP^d/PrP^{res}, clinical disease and infectious titre in classical TSEs, it is necessary to suggest that key toxic and putative infectious forms of PrP escape detection by all current detection methods. In this context it should be recognised that PrP^d detected by immunohistochemistry is not limited to protease-resistant forms of PrP [54].

It has been clearly shown that PrP^c is required for infection [15] and that gene dosage of PrP^c affects incubation period [111]. Morphological data support the idea that PrP^d can be toxic while experimental data suggest that removing PrP^c may be protective in the presence of a scrapie-like infection, but it is not at all clear that PrP^d is essential for initiating clinical signs, at least under natural disease conditions. The literature contains many false syllogisms: the fact that PrP^d/PrP^{res} is present in most brains of classical TSE-affected individuals, and that transmission can be achieved from most TSE-affected tissues does not inevitably lead to the conclusion that PrP^d/PrP^{res} is either the infectious agent or the proximate cause of disease. While there is evidence to show that infectivity may be generated de novo from synthetic forms of PrP^c and poly(A) RNA [36], that is, infectivity can be generated from starting components that lack PrP^{res}, the output infectivity is accompanied by PrP^{res} detectable by Western blotting. Thus, at present there do not appear to be methodologies capable of detecting abnormal forms of PrP that are infectious yet have the capacity to evade current PrP^d/PrP^{res} detection systems.

Conclusions/summary

The nature and morphologic range of PrP^d accumulations found in animal TSEs is extensive. Nevertheless, when disease characteristics are compared across different animals, species and strains there are a number of common sub-cellular changes. While some TSE-specific sub-cellular lesions co-localise with PrP^d, two TSE-specific changes do not. Long recognised tubulovesicular structures and vacuoles remain important changes, which continue to lack, respectively, a molecular definition or pathogenetic understanding.

Chronic human neurodegenerative diseases that are caused by protein aggregation are not thought to be caused primarily by large aggregates of toxic proteins. It is now thought that large aggregates are inert and safer forms of the protein, but small molecular aggregates are more biologically active and toxic. It has similarly been proposed that small molecular aggregates of PrP^d are more toxic than larger aggregates. Consistent with this hypothesis, visibly aggregated forms of PrP^d are rare or absent in most ruminant prion diseases while PrP^d accumulations that are not visibly aggregated are widespread and abundant. Most PrP^d accumulations in ruminant prion diseases are associated with membranes. The aggregate size of PrP^d within membranes cannot be determined by examination in the electron microscope, but aggregates must be small enough to be retained within the structure of plasma membranes. Such monomeric or oligomeric membrane aggregates of PrP^d co-localise with toxic changes of membranes.

PrP^d-associated and TSE-specific membrane pathology is a consistent feature of all animal TSEs. These PrP^d-associated membrane changes are primarily found on dendritic membranes in contrast to the normal partitioning of PrP^c to detergent-resistant lipid-rich segments of axonal membranes. Different molecular partners can be inferred to interact with PrP^d, suggesting it forms multi-molecular complexes with other membrane molecules. These putative PrP^d-protein complexes are poorly excised from the plasma membrane. Whatever the mechanisms by which PrP^d is stabilised within membranes, its preferential distribution to dendrites has implications for membrane composition and physiology. The mechanisms by which PrP^d increases its stability within the membrane and the interrelation between

PrP^c trafficking and PrP^d formation require further exploration, including in the atypical forms of animal prion diseases. Large visibly aggregated forms of PrP^d are found mainly in rodent prion strains. Such fibrillar or amorphous aggregates of PrP^d do not damage membranes although they are associated with other changes, most conspicuously, neuronal dystrophia. Irrespective of the nature of the PrP^d accumulations, when different forms of scrapie are compared both within and between species it is not possible to find any pattern of PrP^d accumulations corresponding to either small or large molecular aggregates that consistently correlates with clinical disease.

As with other chronic neurodegenerative diseases many secondary lesions occur in later stages of animal TSEs. Studying end-stage lesions, such as the mechanism of neuronal death, are unlikely to lead to radical therapeutic improvement or to understanding primary disease pathogenesis. Although TSE-specific membrane pathology provides direct evidence of a "gain of function" (PrP^d toxicity), the nature and extent of PrP^d accumulation when examined across different species, strains and models suggest that PrP^d may not be the proximate cause of clinical neurological disease. Early axon terminal degeneration—which lacks any simple correlation with PrP^d accumulation—provides a strong candidate lesion for clinical disease progression in mice. Further studies of lesions at early stages of infection and better correlation with clinical signs in this and other animal species are needed to investigate the contribution of PrP^d-related and non-PrP^d-related disease mechanisms.

References

1. Asuni AA, Cunningham C, Vigneswaran P, Perry VH, O'Connor V (2008) Unaltered SNARE complex formation in an in vivo model of prion disease. Brain Res 1233:1–7
2. Baker HF, Duchen LW, Jacobs JM, Ridley RM (1990) Spongiform encephalopathy transmitted experimentally from Creutzfeldt-Jakob and familial Gerstmann–Sträussler–Scheinker Diseases. Brain 113:1891–1909
3. Baringer JR, Prusiner SB, Wong JS (1981) Scrapie-associated particles in postsynaptic processes. J Neuropathol Exp Neurol 40:281–288
4. Baron T, Bencsik A, Vulin J et al (2008) A C-terminal protease-resistant prion fragment distinguishes ovine "CH1641-like" scrapie from bovine classical and l-type BSE in ovine transgenic mice. PLoS Pathog 4:e1000137
5. Barron RM, Campbell SL, King D et al (2007) High titers of transmissible spongiform encephalopathy infectivity associated with extremely low levels of PrPSc in vivo. J Biol Chem 282:35878–35886
6. Bastian FO (1979) Spiroplasma-like inclusions in Creutzfeldt–Jakob disease. Arch Pathol Lab Med 103:665–669
7. Beck E, Daniel PM, Davey AJ, Gajdusek DC, Gibbs CJ Jr (1982) The pathogenesis of transmissible spongiform encephalopathy an ultrastructural study. Brain 105:755–786
8. Begara-McGorum I, González L, Simmons M, Hunter N, Houston F, Jeffrey M (2002) Vacuolar lesion profile in sheep scrapie: Factors influencing its variation and relationship to disease-specific PrP accumulation. J Comp Pathol 127:59–68
9. Belichenko PV, Brown D, Jeffrey M, Fraser JR (2000) Dendritic and synaptic alterations of hippocampal pyramidal neurones in scrapie-infected mice. Neuropathol Appl Neurobiol 26:143–149
10. Belichenko PV, Miklossy J, Belser B, Budka H, Celio MR (1999) Early destruction of the extracellular matrix around parvalbumin-immunoreactive interneurons in Creutzfeldt–Jakob disease. Neurobiol Dis 6:269–279
11. Benestad SL, Sarradin P, Thu B, Schonheit J, Tranulis MA, Bratberg B (2003) Cases of scrapie with unusual features in Norway and designation of a new type, Nor98. Vet Rec 153:202–208
12. Bessen RA, Marsh RF (1992) Identification of two biologically distinct strains of transmissible mink encephalopathy in hamsters. Gen Virol 73:329–334
13. Bouzamondo Bernstein E, Hopkins SD, Spilman P et al (2004) The neurodegeneration sequence in prion diseases: Evidence from functional, morphological and ultrastructural studies of the GABAergic system. J Neuropathol Exp Neurol 63:882–899
14. Bradley R (1996) Experimental transmission of bovine spongiform encephalopathy. In: Court L, Dodet B (eds) Transmissible subacute spongiform encephalopathies: prion diseases. Elsevier Editions Scientifiques, Paris, pp 51–56
15. Brandner S, Isenmann S, Raeber A et al (1996) Normal host prion protein necessary for scrapie-induced neurotoxicity. Nature 379:339–343
16. Brown D, Belichenko P, Sales J, Jeffrey M, Fraser AR (2001) Early loss of dendritic spines in murine scrapie revealed by confocal analysis. Neuroreport 12:179–183
17. Bruce ME, McBride PA, Farquhar CF (1989) Precise targeting of the pathology of the sialoglycoprotein PrP, and vacuolar degeneration in mouse scrapie. Neurosci Lett 102:1–6
18. Bruce M, Chree A, McConnell I, Foster J, Pearson G, Fraser H (1994) Transmission of bovine spongiform encephalopathy and scrapie to mice: strain variation and the species barrier. Phil Trans Roy Soc Lond B 343:405–411
19. Bruce M, Chree A, Williams ES, Fraser H (2000) Perivascular PrP amyloid in the brains of mice infected with chronic wasting disease. Brain Pathol 10:662–663
20. Bruce ME (1993) Scrapie strain variation and mutation. Br Med Bull 49:822–839
21. Bruce ME, Fraser H (1991) Scrapie strain variation and its implications. Curr Top Microbiol Immunol 172:125–138
22. Buschmann A, Gretzschel A, Biacabe AG et al (2006) Atypical BSE in Germany-proof of transmissibility and biochemical characterization. Vet Microbiol 117:103–116
23. Carlson GA, Westaway D, DeArmond SJ, Peterson-Torchia M, Prusiner SB (1989) Primary structure of prion protein may modify scrapie isolate properties. Proc Natl Acad Sci USA 86:7475–7479
24. Casalone C, Caramelli M, Crescio MI, Spencer YI, Simmons MM (2006) BSE immunohistochemical patterns in the brainstem: a comparison between UK and Italian cases. Acta Neuropathol 111:444–449
25. Casalone C, Zanusso G, Acutis P et al (2004) Identification of a second bovine amyloidotic spongiform encephalopathy: Molecular similarities with sporadic Creutzfeldt–Jakob disease. Proc Nat Acad Sci USA 101:3065–3070
26. Caughey B, Baron GS, Chesebro B, Jeffrey M (2009) Getting a grip on prions: oligomers, amyloids, and pathological membrane interactions. Annu Rev Biochem 78:177–204
27. Caughey B, Raymond GJ, Ernst D, Race RE (1991) N-Terminal truncation of the scrapie-associated form of PrP by lysosomal

protease(s): implications regarding the site of conversion of PrP to the protease-resistant state. J Virol 65:6597–6603
28. Chesebro B, Race B, Meade-White K et al. (2010) Fatal transmissible amyloid encephalopathy: a new type of prion disease associated with lack of prion protein membrane anchoring. PLoS Pathog 6(3):e1000800
29. Chesebro B, Trifilo M, Race R et al (2005) Anchorless prion protein results in infectious amyloid disease without clinical scrapie. Science 308:1435–1439
30. Chiesa R, Piccardo P, Ghetti B, Harris DA (1999) A transgenic mouse model of a familial prion disease with an insertional mutation. In: Iqbal K, Swaab DF, Winblad B, Wisniewski HM (eds) Alzheimers disease and related disorders. Wiley, West Sussex, pp 569–580
31. Chiesa R, Piccardo P, Quaglio E et al (2003) Molecular distinction between pathogenic and infectious properties of the prion protein. J Virol 77:7611–7622
32. Cunningham AA, Kirkwood JK, Dawson M, Spencer YI, Green RB, Wells GAH (2004) Bovine Spongiform encephalopathy infectivity in greater kudu (*Tragelaphus strepsiceros*). Emerg Infect Dis 10:1044–1048
33. Cunningham C, Deacon R, Wells H et al (2003) Synaptic changes characterize early behavioural signs in the ME7 model of murine prion disease. Eur J Neurosci 17:2147–2155
34. David-Farreira JF, David-Farreira KL, Gibbs CJ (1968) Scrapie in mice: ultrastructural observations in the cerebral cortex. Proc Soc Exp Biol Med 127:313–320
35. DeArmond SJ, McKinley MP, Barry RA, Braunfeld MB, McColloch JR, Prusiner SB (1985) Identification of prion amyloid filaments in scrapie-infected brain. Cell 41:221–235
36. Deleault NR, Harris BT, Rees JR, Supattapone S (2007) Formation of native prions from minimal components in vitro. Proc Natl Acad Sci USA 104:9741–9746
37. Dickinson AG (1976) Scapie in sheep and goats. In: Kimberlin RH (ed) Slow virus diseases of animals and man. North Holland, Amsterdam, pp 209–241
38. Diedrich JF, Bendheim PE, Kim YS, Carp RI, Haase AT (1991) Scrapie-associated prion protein accumulates in astrocytes during scrapie infection. Proc Nat Acad Sci USA 88:375–379
39. Doerr-Schott J, Kitamoto T, Tateishi J, Boellaard JW, Heldt N, Lichte C (1990) Immunogold light and electron microscopic detection of amyloid plaques in transmissible spongiform encephalopathies. Neuropathol Appl Neurobiol 16:85–89
40. Ersdal C, Goodsir CM, Simmons MM, McGovern G, Jeffrey M (2009) Abnormal prion protein is associated with changes of plasma membranes and endocytosis in bovine spongiform encephalopathy (BSE)-affected cattle brains. Neuropathol Appl Neurobiol 35:259–271
41. Ersdal C, Simmons MM, González L, Goodsir CM, Martin S, Jeffrey M (2004) Relationships between ultrastructural scrapie pathology and patterns of abnormal prion protein accumulation. Acta Neuropathol 107:428–438
42. Ersdal C, Simmons MM, Goodsir C, Martin S, Jeffrey M (2003) Sub-cellular pathology of scrapie: coated pits are increased in PrP codon 136 alanine homozygous scrapie-affected sheep. Acta Neuropathol 106:17–28
43. Ersdal C, Ulvund MJ, Benestad SL, Tranulis MA (2003) Accumulation of pathogenic prion protein (PrP^{Sc}) in nervous and lymphoid tissues of sheep with subclinical scrapie. Vet Pathol 40:164–174
44. Fevrier B, Vilette D, Archer F et al (2004) Cells release prions in association with exosomes. Proc Nat Acad Sci USA 101:9683–9688
45. Flechsig E, Shmerling D, Hegyi I et al (2000) Prion protein devoid of the octapeptide repeat region restores susceptibility to scrapie in PrP knockout mice. Neuron 27:399–408
46. Forloni G, Angeretti N, Chiesa R et al (1993) Neurotoxicity of a prion protein fragment. Nature 362:543–546
47. Fuhrmann M, Mitteregger G, Kretzschmar H, Herms J (2007) Dendritic pathology in prion disease starts at the synaptic spine. J Neurosci 27:6224–6233
48. Galvan C, Camoletto PG, Dotti CG, Aguzzi A, Ledesma MD (2005) Proper axonal distribution of PrP(C) depends on cholesterol-sphingomyelin-enriched membrane domains and is developmentally regulated in hippocampal neurons. Mol Cell Neurosci 30:304–315
49. Giaccone GG, Verga L, Bugiani O et al (1992) Prion protein preamyloid and amyloid deposits in Gerstmann–Straussler–Scheinker disease, Indiana kindred. Proc Nat Acad Sci USA 89:9349–9353
50. Godsave SF, Wille H, Kujala P et al (2008) Cryo-Immunogold electron microscopy for prions: toward identification of a conversion site. J Neurosci 28:12489–12499
51. González L, Martin S, Begara McGorum I et al (2002) Effects of agent strain and host genotype on PrP accumulation in the brain of sheep naturally and experimentally affected with scrapie. J.Comp Pathol 126:17–29
52. González L, Martin S, Houston FE et al (2005) Phenotype of disease-associated PrP accumulation in the brain of bovine spongiform encephalopathy experimentally infected sheep. J Gen Virol 86:827–838
53. González L, Martin S, Jeffrey M (2003) Distinct profiles of PrP^{d} immunoreactivity in the brain of scrapie-and BSE-infected sheep: implications for differential cell targeting and PrP processing. J Gen Virol 84:1339–1350
54. González L, Terry L, Jeffrey M (2005) Expression of prion protein in the gut of mice infected orally with the 301v murine strain of the bovine spongiform encephalopathy agent. J Comp Pathol 132:273–282
55. Gray A, Francis RJ, Scholtz CL (1980) Spiroplasma and Creutzfeldt–Jakob disease. Lancet 2:152
56. Gray BC, Siskova Z, Perry VH, O'Connor V (2009) Selective presynaptic degeneration in the synaptopathy associated with ME7-induced hippocampal pathology. Neurobiol Dis 35:63–74
57. Green KM, Browning SR, Seward TS et al (2008) The elk PRNP codon 132 polymorphism controls cervid and scrapie prion propagation. J Gen Virol 89:598–608
58. Groschup MH, Weiland F, Straub OC, Pfaff E (1996) Detection of scrapie agent in the peripheral nervous system of a diseased sheep. Neurobiol Dis 3:191–195
59. Haeberle AM, Ribaut Barassin C, Bombarde G et al (2000) Synaptic prion protein immuno-reactivity in the rodent cerebellum. Microsc Res Technique 50:66–75
60. Harris DA (2003) Trafficking, turnover and membrane topology of PrP. Br Med Bull 66:71
61. Hope J, Wood SCER, Birkett CR et al (1999) Molecular analysis of ovine prion protein identifies similarities between BSE and an experimental isolate of natural scrapie, CH1641. J Gen Virol 80:1–4
62. Hunter N (1991) Scrapie and GSS—Gerstmann–Straussler–Scheinker syndrome—the importance of protein. Trends Neurosci 14:389–390
63. Ilangumaran S, Robinson PJ, Hoessli DC (1996) Transfer of exogenous glycosylphos-phatidylinositol (GPI)-linked molecules to plasma membranes. Trends Cell Biol 6:163–167
64. Jacobs JG, Langeveld JP, Biacabe AG et al (2007) Molecular discrimination of atypical bovine spongiform encephalopathy strains from a geographical region spanning a wide area in Europe. J Clin Microbiol 45:1821–1829
65. Jeffrey M, Fraser JR (2000) Tubulovesicular particles occur early in the incubation period of murine scrapie. Acta Neuropathol 99:525–528

66. Jeffrey M, Fraser JR, Halliday WG, Fowler N, Goodsir CM, Brown DA (1995) Early unsuspected neuron and axon terminal loss in scrapie-infected mice revealed by morphometry and immunocytochemistry. Neuropathol Appl Neurobiol 21:41–49
67. Jeffrey M, González L, Chong A et al (2006) Ovine infection with the agents of scrapie (CH1641 isolate) and bovine spongiform encephalopathy: immunochemical similarities can be resolved by immunohistochemistry. J Comp Pathol 134:17–29
68. Jeffrey M, Goodsir CM, Bruce ME, McBride PA, Scott JR, Halliday WG (1992) Infection specific prion protein (PrP) accumulates on neuronal plasmalemma in scrapie infected mice. Neurosci Lett 147:106–109
69. Jeffrey M, Goodsir C, McGovern G, Barmada SJ, Medrano AZ, Harris DA (2009) Prion protein with an insertional mutation accumulates on axonal and dendritic plasmalemma and is associated with distinctive ultrastructural changes. Am J Pathol 175:1208–1217
70. Jeffrey M, Goodsir CM, Bruce ME, McBride PA (1993) Infection specific prion protein (PrP) accumulates on neuronal plasmalemma in scrapie infected mice [Abstract]. Neuropathol Appl Neurobiol 19:188
71. Jeffrey M, Goodsir CM, Bruce ME, McBride PA, Farquhar C (1994) Morphogenesis of amyloid plaques in 87V murine scrapie. Neuropathol Appl Neurobiol 20:535–542
72. Jeffrey M, Goodsir CM, Bruce ME, McBride PA, Fraser JR (1996) Subcellular localization and toxicity of pre-amyloid and fibrillar prion protein accumulations in murine scrapie. In: Court L, Dodet B (eds) Transmissible subacute spongiform encephalopathies: prion diseases. Elsevier Editions Scientifiques, Paris, pp 129–135
73. Jeffrey M, Goodsir CM, Bruce ME, McBride PA, Fraser JR (1997) In vivo toxicity of prion protein in murine scrapie: Ultrastructural and immunogold studies. Neuropathol Appl Neurobiol 23:93–101
74. Jeffrey M, Goodsir CM, Bruce ME, McBride PA, Scott JR, Halliday WG (1994) Correlative light and electron microscopy studies of PrP localisation in 87V scrapie. Brain Res 656:329–343
75. Jeffrey M, Goodsir CM, Fowler N, Hope J, Bruce ME, McBride PA (1996) Ultrastructural immuno-localization of synthetic prion protein peptide antibodies in 87V murine scrapie. Neurodegeneration 5:101–109
76. Jeffrey M, Goodsir CM, Holliman A et al (1998) Determination of the frequency and distribution of vascular and parenchymal amyloid with polyclonal and N-terminal-specific PrP antibodies in scrapie-affected sheep and mice. Vet Rec 142:534–537
77. Jeffrey M, Goodsir CM, Race RE, Chesebro B (2004) Scrapie-specific neuronal lesions are independent of neuronal PrP expression. Ann Neurol 55:781–792
78. Jeffrey M, Halliday WG, Bell J et al (2000) Synapse loss associated with abnormal PrP precedes neuronal degeneration in the scrapie-infected murine hippocampus. Neuropathol Appl Neurobiol 26:41–54
79. Jeffrey M, Halliday W (1994) Numbers of neurons in vacuolated and non vacuolated neuroanatomical nuclei in bovine spongiform encephalopathy affected brains. J Comp Pathol 110:287–293
80. Jeffrey M, Martin S, González L (2003) Cell-associated variants of disease-specific prion protein immunolabelling are found in different sources of sheep transmissible spongiform encephalopathy. J Gen Virol 84:1033–1046
81. Jeffrey M, Martin S, González L et al (2006) Immunohistochemical features of $Prp^{(d)}$ accumulation in natural and experimental goat transmissible spongiform encephalopathies. J Comp Pathol 134:171–181
82. Jeffrey M, Martin S, González L, Ryder SJ, Bellworthy SJ, Jackman R (2001) Differential diagnosis of infections with the bovine spongiform encephalopathy (BSE) and scrapie agents in sheep. J Comp Pathol 125:271–284
83. Jeffrey M, McGovern G, Goodsir CM, González L (2009) Strain-associated variations in abnormal PrP trafficking of sheep scrapie. Brain Pathol 19:1–11
84. Jeffrey M, Scott JR, Williams A, Fraser H (1992) Ultrastructural features of spongiform encephalopathy transmitted to mice from three species of bovidae. Acta Neuropathol 84:559–569
85. Jeffrey M, Wells GA (1988) Spongiform encephalopathy in a nyala (*Tragelaphus angasi*). Vet Pathol 25:398–399
86. Johnston AR, Fraser JR, Jeffrey M, Macleod N (1998) Alterations in potassium currents may trigger neurodegeneration in murine scrapie. Exp Neurol 151:326–333
87. Kazlauskaite J, Sanghera N, Sylvester I, Venien-Bryan C, Pinheiro TJT (2003) Structural changes of the prion protein in lipid membranes leading to aggregation and fibrillization. Biochemistry 42:3295–3304
88. Kirkwood JK, Cunningham AA, Flach EJ, Thornton SM, Wells GAH (1995) Spongiform encephalopathy in another captive cheetah (*Acinonyx jubatus*)—evidence for variation in susceptibility or incubation periods between species. J Zoo Wildl Med 26:577–582
89. Konold T, Bone G, Vidal-Diez A et al (2008) Pruritus is a common feature in sheep infected with the BSE agent. BMC Vet Res 4:16
90. Kovacs GG, Budka H (2008) Prion diseases: from protein to cell pathology. Am J Pathol 172:555–565
91. Kovacs GG, Gelpi E, Strobel T et al (2007) Involvement of the endosomal–lysosomal system correlates with regional pathology in Creutzfeldt–Jakob disease. J Neuropathol Exp Neurol 66:628–636
92. Laine J, Marc ME, Sy MS, Axelrad H (2001) Cellular and subcellular morphological localization of normal prion protein in rodent cerebellum. Eur J Neurosci 14:47–56
93. Lasmézas CI, Deslys JP, Robain O et al (1997) Transmission of the BSE agent to mice in the absence of detectable abnormal prion protein. Science 275:402–405
94. Lezmi S, Bencsik A, Monks E, Petit T, Baron T (2003) First case of feline spongiform encephalopathy in a captive cheetah born in France: PrP^{sc} analysis in various tissues revealed unexpected targeting of kidney and adrenal gland. Histochem Cell Biol 119:415–422
95. Liberski PP, Brown DR, Sikorska B, Caughey B, Brown P (2008) Cell death and autophagy in prion diseases (transmissible spongiform encephalopathies). Folia Neuropathol 46:1–25
96. Liberski PP, Budka H, Yanagihara R, Gibbs CJ, Gajdusek DC (1993) Tubulovesicular structures. Light and electron microscopic neuropathology of slow virus disorders. CRC Press, Florida, pp 373–392
97. Liberski PP, Guiroy DC, Williams ES, Walis A, Budka H (2001) Deposition patterns of disease-associated prion protein in captive mule deer brains with chronic wasting disease. Acta Neuropathol 102:496–500
98. Liberski PP, Jeffrey M, Goodsir C (1997) Tubulovesicular structures are not labeled using antibodies to prion protein (PrP) with the immunogold electron microscopy techniques. Acta Neuropathol 93:260–264
99. Liberski PP, Sikorska B, Guiroy D, Bessen RA (2009) Transmissible mink encephalopathy—review of the etiology of a rare prion disease. Folia Neuropathol 47:195–204
100. Liberski PP, Sikorska B, Hauw JJ et al (2008) Tubulovesicular structures are a consistent (and unexplained) finding in the brains of humans with prion diseases. Virus Res 132:226–228

101. Liberski PP, Streichenberger N, Giraud P et al (2005) Ultrastructural pathology of prion diseases revisited: brain biopsy studies. Neuropathol Appl Neurobiol 31:88–96
102. Liberski PP, Yanagihara R, Gibbs CJ Jr, Gajdusek DC (1990) Appearance of tubulovesicular structures in experimental Creutzfeldt–Jakob disease and scrapie precedes the onset of clinical disease. Acta Neuropathol 79:349–354
103. Linden R, Martins VR, Prado MA, Cammarota M, Izquierdo I, Brentani RR (2008) Physiology of the prion protein. Physiol Rev 88:673–728
104. Liu T, Li RL, Pan T et al (2002) Intercellular transfer of the cellular prion protein. J Biol Chem 277:47671–47678
105. Lowe J, Fergusson J, Kenward N et al (1992) Immunoreactivity to ubiquitin-protein conjugates is present early in the disease process in the brains of scrapie-infected mice. Pathology 168:169–177
106. Luhr KM, Nordstrom EK, Low P, Kristensson K (2004) Cathepsin B and L are involved in degradation of prions in GTI-1 neuronal cells. Neuroreport 15:1663–1667
107. Lyahyai J, Bolea R, Serrano C et al (2006) Correlation between Bax overexpression and prion deposition in medulla oblongata from natural scrapie without evidence of apoptosis. Acta Neuropathol 112:451–460
108. Mackenzie A (1983) Immunohistochemical demonstration of glial fibrillary acidic protein in scrapie. J Comp Pathol 93:251–259
109. Madore N, Smith KL, Graham CH et al (1999) Functionally different GPI proteins are organized in different domains on the neuronal surface. EMBO J 18:6917–6926
110. Mallucci G, Dickinson A, Linehan J, Klohn PC, Brandner S, Collinge J (2003) Depleting neuronal PrP in prion infection prevents disease and reverses spongiosis. Science 302:871–874
111. Manson JC, Clarke AR, McBride PA, McConnell I, Hope J (1994) PrP gene dosage determines the timing but not the final intensity or distribution of lesions in scrapie pathology. Neurodegeneration 3:331–340
112. Manuelidis L (2004) A virus behind the mask of prions? Folia Neuropathol 42(Suppl B):10–23
113. Marsh RF, Hadlow WJ (1992) Transmissible mink encephalopathy. Revue Scientifique et Technique Office International des Epizooties 11:539–550
114. Marsh RF, Sipe JC, Morse SS, Hanson RP (1976) Transmissible mink encephalopathy: reduced spongiform degeneration in aged mink of the Chediak–Higashi genotype. Lab Invest 34:381–386
115. Martin S, González L, Chong A, Houston FE, Hunter N, Jeffrey M (2005) Immunohistochemical characteristics of disease-associated PrP are not altered by host genotype or route of inoculation following infection of sheep with bovine spongiform encephalopathy. J Gen Virol 86:839–848
116. Martin S, Jeffrey M, González L et al (2009) Immunohistochemical and biochemical characteristics of BSE and CWD in experimentally infected European red deer (*Cervus elaphus elaphus*). BMC Vet Res 5:26
117. McBride PA, Wilson MI, Eikelenboom P, Tunstall A, Bruce ME (1998) Heparan sulfate proteoglycan is associated with amyloid plaques and neuroanatomically targeted PrP pathology throughout the incubation period of scrapie-infected mice. Exp Neurol 149:447–454
118. McGovern G, Jeffrey M (2007) Scrapie-specific pathology of sheep lymphoid tissues. PLoS ONE 2:e1304
119. McGovern G, Mabbott N, Jeffrey M (2009) Scrapie affects the maturation cycle and immune complex trapping by follicular dendritic cells in mice. PLoS ONE 4:e8186
120. Medrano AZ, Barmada SJ, Biasini E, Harris DA (2008) GFP-tagged mutant prion protein forms intra-axonal aggregates in transgenic mice. Neurobiol Dis 31:20–32
121. Miller MW, Williams ES (2004) Chronic wasting disease of cervids. In: Harris D (ed) Mad cow disease and related spongiform encephalopathies. Springer, Berlin, pp 193–214
122. Mironov A Jr, Latawiec D, Wille H et al (2003) Cytosolic prion protein in neurons. J Neurosci 23:7183–7193
123. Moore SJ, Simmons M, Chaplin M, Spiropoulos J (2008) Neuroanatomical distribution of abnormal prion protein in naturally occurring atypical scrapie cases in Great Britain. Acta Neuropathol 116:547–559
124. Moya KL, Hassig R, Creminon C, Laffont I, DiGiamberardino L (2004) Enhanced detection and retrograde axonal transport of PrP^c in peripheral nerve. J Neurochem 88:155–160
125. Moya KL, Sales N, Hassig R, Creminon C, Grassi J, Di Giamberardino L (2000) Immunolocalization of the cellular prion protein in normal brain. Microsc Res Tech 50:58–65
126. Pearson G, Wyatt J, Henderson J, Gruffydd-Jones T (1993) Feline spongiform encephalopathy: a review. Vet Annu 33:1–10
127. Piccardo P, Manson JC, King D, Ghetti B, Barron RM (2007) Accumulation of prion protein in the brain that is not associated with transmissible disease. Proc Natl Acad Sci USA 104:4712–4717
128. Prusiner SB (1991) Molecular biology and transgenetics of prions causing CNS degeneration of humans and animals. In: Bradley R et al. (eds) Sub-acute spongiform encephalopathies. EEC Brussels and Luxembourg, pp 59–82
129. Prusiner SB, Kaneko K, Serban H, Cohen FE, Safar J, Riesner D (1999) Some strategies and methods for the study of prions. In: Prusiner SB (ed) Prion biology and diseases. Cold Spring Harbor Laboratory Press, New York, pp 653–715
130. Race R, Raines A, Raymond GJ, Caughey B, Chesebro B (2001) Long-term subclinical carrier state precedes scrapie replication and adaptation in a resistent species: analogies to bovine spongiform encephalopathy and variant Creutzfeldt–Jakob disease in humans. J Virol 75:10106–10112
131. Raeber AJ, Race RE, Brandner S et al (1997) Astrocyte-specific expression of hamster prion protein (PrP) renders PrP knockout mice susceptible to hamster scrapie. EMBO J 16:6057–6065
132. Revesz T, Holton JL, Lashley T et al (2009) Genetics and molecular pathogenesis of sporadic and hereditary cerebral amyloid angiopathies. Acta Neuropathol 118:115–130
133. Rodolfo K, Hassig R, Moya KL, Frobert Y, Grassi J, Di Giamberardino L (1999) A novel cellular prion protein isoform present in rapid anterograde axonal transport. Neuroreport 10:3639–3644
134. Rodríguez A, Martin M, Albasanz JL et al (2006) Group I mGluR signaling in BSE-infected bovine-PrP transgenic mice. Neurosci Lett 410:115–120
135. Sales N, Hassig R, Rodolfo K et al (2002) Developmental expression of the cellular prion protein in elongating axons. Eur J Neurosci 15:1163–1177
136. Serrano C, Lyahyai J, Bolea R et al (2009) Distinct spatial activation of intrinsic and extrinsic apoptosis pathways in natural scrapie: association with prion-related lesions. Vet Res 40:42
137. Shyng SL, Moulder KL, Lesko A, Harris DA (1995) The N-terminal domain of a glycolipid-anchored prion protein is essential for its endocytosis via clathrin-coated pits. J Biol Chem 270:14793–14800
138. Siskova Z, Page A, O'Connor V, Perry VH (2009) Degenerating synaptic boutons in prion disease. Am J Pathol 175:1610–1621
139. Sisó S, Doherr MG, Botteron C et al (2007) Neuropathological and molecular comparison between clinical and asymptomatic bovine spongiform encephalopathy cases. Acta Neuropathol 114:501–508
140. Sisó S, Ordóñez M, Cordón I, Vidal E, Pumarola M (2004) Distribution of PrP^{res} in the brains of BSE-affected cows

detected by active surveillance in Catalonia, Spain. Vet Rec 155:524–525
141. Sisó S, Puig B, Varea R et al (2002) Abnormal synaptic protein expression and cell death in murine scrapie. Acta Neuropathol 103:615–626
142. Snow AD, Wight TN, Nochlin D et al (1990) Immunolocalization of heparan sulfate proteoglycans to the prion protein amyloid plaques of Gerstmann–Straussler syndrome, Creutzfeldt–Jakob disease and scrapie. Lab Invest 63:601–611
143. Spiropoulos J, Casalone C, Caramelli M, Simmons MM (2007) Immunohistochemistry for PrP^{Sc} in natural scrapie reveals patterns which are associated with the PrP genotype. Neuropathol Appl Neurobiol 33:398–409
144. Spraker TR, Zink RR, Cummings BA, Wild MA, Miller MW, O'Rourke KI (2002) Comparison of histological lesions and immunohistochemical staining of proteinase-resistant prion protein in a naturally occurring spongiform encephalopathy of free-ranging mule deer (*Odocoileus hemionus*) with those of chronic wasting disease of captive mule deer. Vet Pathol 39:110–119
145. Stack M, Jeffrey M, Gubbins S et al (2006) Monitoring for bovine spongiform encephalopathy in sheep in Great Britain, 1998–2004. J Gen Virol 87:2099–2107
146. Stack MJ, Chaplin MJ, Clark J (2002) Differentiation of prion protein glycoforms from naturally occurring sheep scrapie, sheep-passaged scrapie strains (CH1641 and SSBP1), bovine spongiform encephalopathy (BSE) cases and Romney and Cheviot breed sheep experimentally inoculated with BSE using two monoclonal antibodies. Acta Neuropathol 104:279–286
147. Stahl N, Baldwin MA, Burlingame AL, Prusiner SB (1990) Identification of glycoinositol phospholipid linked and truncated forms of the scrapie prion protein. Biochem 29:8879–8884
148. Steele AD, King OD, Jackson WS et al (2007) Diminishing apoptosis by deletion of Bax or overexpression of Bcl-2 does not protect against infectious prion toxicity in vivo. J Neurosci 27:13022–13027
149. Theil D, Fatzer R, Meyer R, Schobesberger M, Zurbriggen A, Vandevelde M (1999) Nuclear DNA fragmentation and immune reactivity in bovine spongiform encephalopathy. J Comp Pathol 121:357–367
150. Van Keulen LJM, Schreuder BEC, Meloen RH et al (1995) Immunohistochemical detection and localization of prion protein in brain tissue of sheep with natural scrapie. Vet Pathol 32:299–308
151. Veith NM, Plattner H, Stuermer CA, Schulz-Schaeffer WJ, Burkle A (2009) Immunolocalisation of PrP^{Sc} in scrapie-infected N2a mouse neuroblastoma cells by light and electron microscopy. Eur J Cell Biol 88:45–63
152. Vella LJ, Sharples RA, Nisbet RM, Cappai R, Hill AF (2008) The role of exosomes in the processing of proteins associated with neurodegenerative diseases. Eur Biophys J 37:323–332
153. Walmsley AR, Zeng F, Hooper NM (2003) The N-terminal region of the prion protein ectodomain contains a lipid raft targeting determinant. J Biol Chem 278:37241–37248
154. Weller RO, Subash M, Preston SD, Mazanti I, Carare RO (2008) Perivascular drainage of amyloid-beta peptides from the brain and its failure in cerebral amyloid angiopathy and Alzheimer's disease. Brain Pathol 18:253–266
155. Wells GAH, Wilesmith JW, McGill IS (1991) Bovine spogiform encephalopathy: a neuropathological perspective. Brain Pathol 1:69–78
156. White MD, Farmer M, Mirabile I, Brandner S, Collinge J, Mallucci GR (2008) Single treatment with RNAi against prion protein rescues early neuronal dysfunction and prolongs survival in mice with prion disease. Proc Natl Acad Sci USA 105:10238–10243